6-18-2009

Alkali activated aerogels

Forrest R. Svingala

Alkali Activated Aerogels

By

Forrest R. Svingala

Department of Mechanical Engineering, Kate Gleason College of Engineering

A thesis accepted for the Degree of Master of Science on June 18th, 2009.

Dr. Benjamin Varela, Advisor

Dr. Edward Hensel, Department Head

Dr. Hany Ghoneim

Dr. Marca Lam

Alkali Activated Aerogels

By

Forrest R. Svingala

A thesis submitted in partial fulfillment of the requirements for the degree of Master of Science in Mechanical Engineering from the Rochester Institute of Technology, Rochester NY.

Abstract:

Clay aerogels are unique materials formed through the sublimation drying of aluminosilicate clay hydrogels. Aerogels have been an area of increased research interest in the past decade due to their very low density, high surface area/porosity, and very low thermal conductivity. Significant efforts have been made to increase the mechanical strength and moisture resistance of these materials through the incorporation of both organic polymers and fiber reinforcement. Aluminosilicates can also be alkali activated, producing a highly-crosslinked 3D network polymer with generally excellent mechanical strength and chemical resistance, but with high density. This work presents a preliminary investigation into the combination of aerogel production techniques with alkali activation, with the goal of producing a high strength, alkali activated aerogel. Metakaolin, dehydroxylated montmorillonite and S-Type furnace slag were investigated as aluminosilicate sources. It was found that it is possible to create a stable solid material with density of approximately 0.9 $g \bullet cm^{-1}$, compressive strength up to 9.9 MPa, and porosity on the order of 10-30 microns.

Acknowledgements:

Any work of this magnitude is not possible without the advice and support of many friends and colleagues. I would like to take this opportunity to thank all those who contributed directly or indirectly to the work herein. Firstly, I would like to thank my advisor, Dr. Varela. Without his vision and guidance this project could not have even began, let alone reached completion. His lighthearted attitude made this process a pleasure. I'd also like to thank Dr. Langner for contributing his time, extensive knowledge, and use of his laboratory over the course of this investigation. I am also indebted to David Fister of CIMS and Professor Richard Hailstone of CIS for the use of their microscopy equipment. Finally, I would like to thank my friends and family for their love, support, and the generous supply of confidence and sanity they gladly contributed when I was in need.

I would also like to thank the Center for Layered Polymeric Structures at Case Western Reserve University for funding and support of this project. This material is based upon work supported by the National Science Foundation under Award No. DMR-0423914

Table of Contents

List of Figures:

List of Tables:

Chapter 1:

Introduction

In the early 1930's Kistler [1] found that a conventional wet gel could be dried without a reduction in volume through a lengthy supercritical drying process. His technique produced very low density, highly porous materials, he called aerogels. Twenty years later, Hoffman [2] and Call [3] showed that an aerogel consisting of montmorillonite clay could be produced using a freeze drying process. This material was exceptional in its extremely low density (0.02- 0.1 $g \bullet cm^{-1}$) and very high porosity. Schirialdi, Gawryla and others have revived interest in this material in recent years as a green substitute for many of the petroleum expanded foams which are ubiquitous in many parts of modern life. Specifically, these materials show promise as lightweight packing materials and insulators. Unfortunately, pure clay areogels rely solely on physical electrostatic bonds for rigidity, and thus have negligible mechanical strength. These materials also reconvert to the wet gel state in high humidity environments. These drawbacks are the focus of much of the current work in the clay aerogel field.

Alkali activated materials, especially Geopolymers, are mechanically the antithesis of the clay aerogel. These materials exhibit much higher densities and mechanical properties similar to portland cement. Alkali activated materials were used as far back as ancient Egypt for casting small statues and vases [4]. Davidovits first patented an alkali activated geopolymer in the 1960's, sparking fresh research into this unique material. Alkali activated materials derive their strength from a framework of polymerized alumina and silica. These materials also have generally excellent chemical and environmental resistance. Research in the geopolymer field is largely focused on the production of a replacement material for conventional concretes for use in the construction industry.

The production of both clay aerogels and geopolymers relies on aluminosilicate materials. In the clay aerogel, the clay is not chemically activated, while in the geopolymer the clay is chemically depolymerized and condensed into a new polymer network. The present work is an investigation into the combination of these two materials, with the goal of creating alkali activated aerogels with greater strength then a pure clay aerogel, and less dense then a geopolymer. These materials will then be characterized based on their mechanical properties, microstructure, infrared spectra, and rheology of the wet material.

Chapter 2:

Literature Review

LITERATURE REVIEW

2.1 Clay Mineralogy

The term 'clay' refers to naturally formed sediment consisting largely of amorphous inorganic particles less than 2 microns in size. In its as mined state, clays often contain significant proportions of larger particles, organic matter, and crystalline remnants of the parent mineral [5]. After mining, the clay is stored to allow bacteria to break down any organic matter present in the clay. Large inorganic particles can be removed mechanically by sieving. Crystalline remnants of the parent mineral are difficult to remove, as their size is often on the order of the clay particles themselves. As such, very purely amorphous clays must be mined from sources with naturally low levels of these associated crystalline phases. Clays are formed by chemical weathering of aluminosilicate minerals, such as feldspars and feldspathoids. Bormans [5] cites several chemical processes responsible for the weathering of minerals into clays. The most common are acidolysis and alkalinolysis, or chemical separation by acidic or alkaline solution, respectively. Salinolysis and hydrolysis, separation by salt solution or by water, respectively, are also mechanisms of chemical weathering. This process produces tetrahedral coordinated sheets of silicon-oxygen and octahedral sheets of magnesium- or aluminum-oxygen-hydroxyl, as shown in Figure 1 [6]. Note that the Si and Al atoms are obscured by the much larger oxygen atoms and hydroxyl groups in this figure.

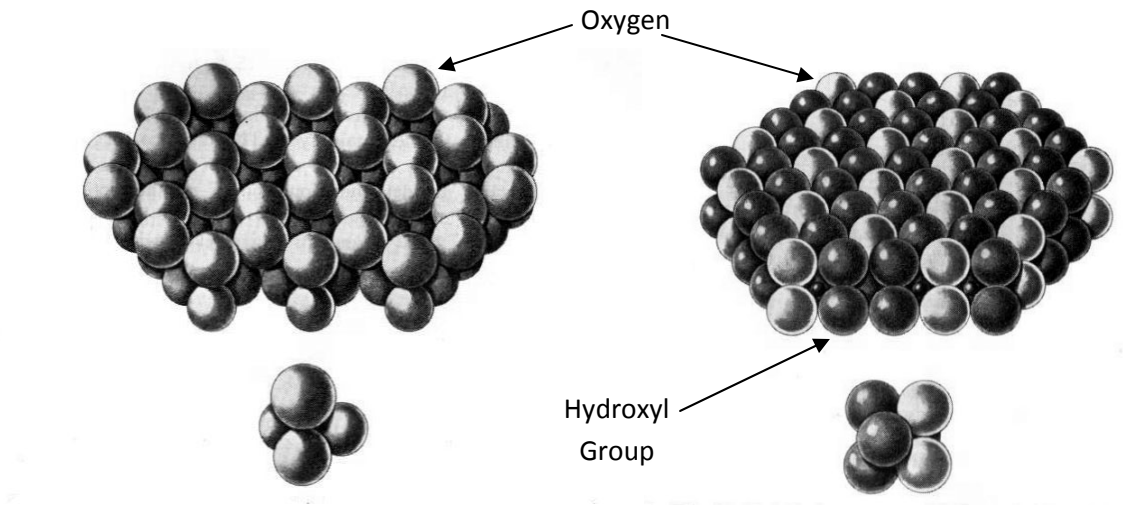

Figure 1: Models of the (a) tetrahedral Silicon-Oxygen sheet and
(b) Octahedral Aluminum-Oxygen-Hydroxyl sheet [6]

Van Olphen [6] notes that isomorphous substitution of trivalent aluminum for tetravalent silicon in the tetrahedral sheet, and divalent magnesium for trivalent aluminum in the octahedral sheet produces an excess of negative charge. This causes the sheets to readily adsorb charge balancing cations, commonly monovalent sodium and potassium. These ions are weakly bonded to the surface of the clay sheet, and are easily exchanged with other available cations in solution. The total amount of these exchangeable cations is commonly expressed in milliequivalents per 100g (meq), which is equal to 1 centimole of unit charge per kilogram ($cmol \bullet Kg^{-1}$). The degree of isomorphous substitution and the physical arrangement of the tetrahedral and octahedral sheets produce many different types of clay. Of these, kaolinite and montmorillonite are of primary importance in the manufacture of clay aerogels and geopolymers.

2.1.1 Kaolinite

Kaolinite clays consist of one silicon tetrahedral sheet and one aluminum octahedral sheet connected through shared oxygen atoms as presented in Figure 2. This structure is known as 1:1 layer clay.

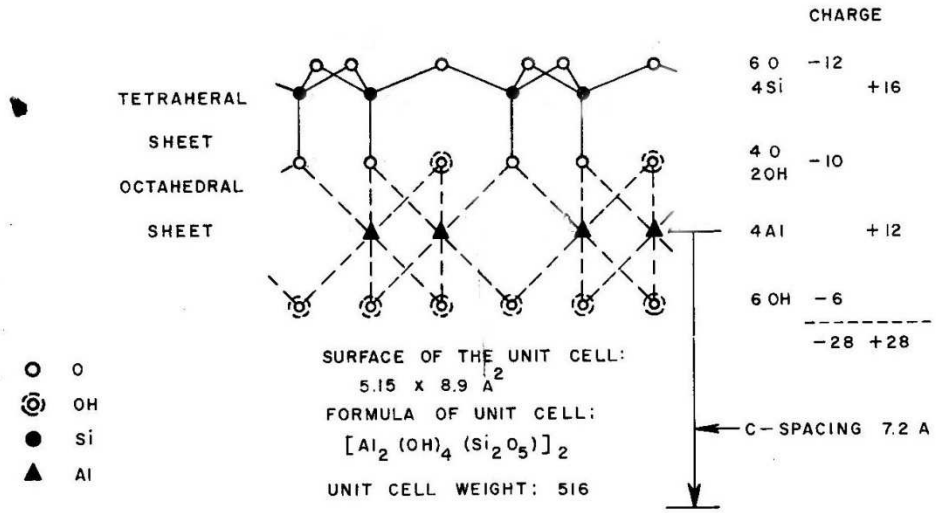

Figure 2: Structure of a 1:1 layer clay [6]

Bond strength in kaolinites is increased due to the presence of both electrostatic bonding between the sheets and hydrogen bonding between the oxygen of the silicon sheet and the hydroxyl of the aluminum sheet. Kaolin exhibits low isomorphous substitution and does not contain any charge compensating cations between the sheets, resulting in a low cation exchange capacity (typically 1-10 meq per 100g) [6]. This lack of interlayer cations also severely limits the ability of molecules to enter and occupy the space between the sheets. Kaolinite is therefore non-expanding in water and most solvents [6]. Clay aerogels using kaolinite have

been demonstrated by Ishikawa et al., but they have generally poor mechanical properties and require much higher solid fractions than those made with montmorillonite clay [7] [8].

2.1.2 Montmorillonite

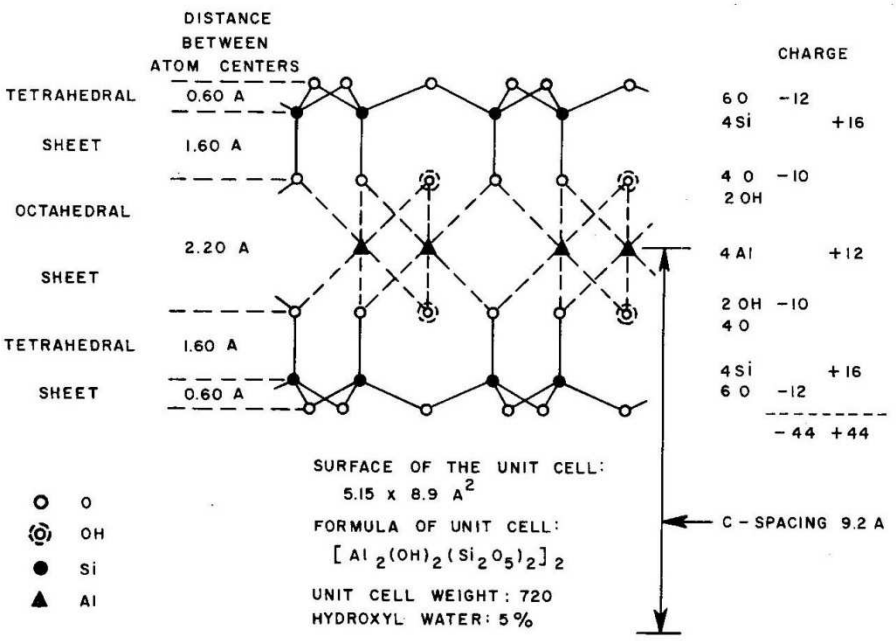

Figure 3: Structure of a 2:1 layer clay [6]

Montmorillonite is 2:1 layer clay, consisting of a single octahedral aluminum sheet sharing oxygen atoms on both sides with tetrahedral silicon sheets. Montmorillonite has a high cation exchange capacity (typically about 70meq per 100g [6]) due to the presence of many interlayer charge compensating cations. The hydration of these cations allows the penetration of up to 4 layers of water molecules between the clay layers, increasing the volume of the clay by up to two times, relative to the dry clay [6]. Sodium ion-exchanged montmorillonite is

commonly used to produce clay aerogels due to its ability to form hydrogels at relatively low solid fractions (5% by weight [9]).

2.2 Clay Aerogels

A conventional gel is a semi-solid material comprised of a solid network with liquid-solvent filled pores. The solid network can consist of a chemically connected polymer network, or a system of physically bonded discrete particles. A physically bonded gel is formed when a liquid-solid colloid is flocculated into a single 'floc' which fills the entire volume of the liquid. The formation of this floc is controlled by electrostatic forces; a gel can only form when the force of repulsion of like-charged solid particles is overcome by van der Waals attraction of those same particles [6].

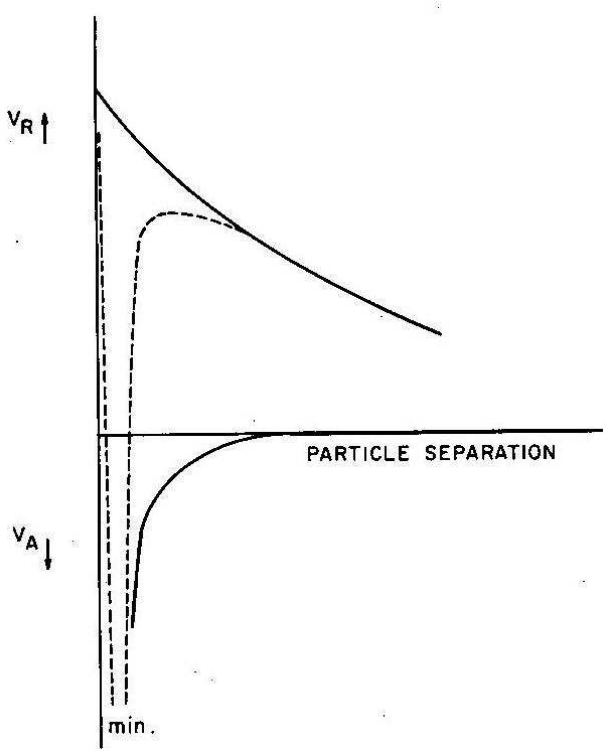

Figure 4: Interaction energy as a function of particle separation. V_R represents repulsive energy, V_A represents attractive energy, and the dashed line represents the sum V_R+V_A

Figure 4 shows the relationship between attractive and repulsive forces as a function of particle separation. At the proper concentration, these particles become trapped in the potential well labeled as 'min.' in the figure below.

In a physically bonded gel, the attraction between solid particles is strong enough to give the liquid-solid system a measure of elasticity and shear strength. In the early 1930s, Kistler [1] found that through a lengthy supercritical drying process, the liquid portion of many liquid-solid gels could be replaced by gas without significant alteration of the network of solid particles. The resulting solid-gas structure, known as an aerogel, has an extremely low density, 0.02- 0.1 $g \bullet cm^{-3}$, greater than 90% porosity, and very low thermal conductivity. Since Kistler's original work with silica and metallic oxides, it has been shown that aerogels can be created from a variety of gels by a number of supercritical and subcritical drying processes.

2.2.1 Creating Clay Aerogels

A method for the creation of aerogels from gelled clay-water colloids was first shown by Hofmann in 1953 [10]. This method was documented in greater detail by Call later that year [2]. The goal of these authors was to produce a dry sample of a clay-water gel suitable for examination under SEM. Conventional drying through evaporation was found to cause significant alteration and shrinkage of the solid structure within the gel. As evaporation proceeds, water from the interior of the gel is drawn to the surface through capillary action. As water moves through the gel, surface tension pulls on the clay particles it passes altering the structure of the gel and causing shrinkage [1]. Hofmann found that clay gels could be dried with a minimal amount of shrinkage through the process of freeze drying. In freeze-drying, the

sample is first frozen, usually in liquid nitrogen or a dry ice/alcohol bath. The sample is then placed in an evacuated environment. Both these actions bring the water present in the sample below its triple point (0 ^{o}C and 4.58 Torr), where the liquid phase of water cannot exist. Under these conditions water is removed through sublimation. With this method of drying, water never enters the liquid phase and so does not change the structure present in the frozen sample.

2.2.2 Structure of Clay Aerogels

While the process of freeze drying is generally accepted to leave the frozen gel unaltered, it has been recently shown that the rate at which a kaolinite clay gel is frozen can alter its structure [7] [8]. Freezing in liquid nitrogen (-196^{o}C) produced an open-cell foam structure that is believed to reflect the structure of the gel before freezing. Freezing at higher temperatures (-30^{o}C and -50^{o}C) allows ice crystals to grow more slowly, altering the position of clay particles in the initial gel. Freezing under these conditions was shown to produce a honeycomb or parallel plate structure, respectively [7]. Figure 5 a-c shows this effect for a 20 %wt kaolinite aerogel.

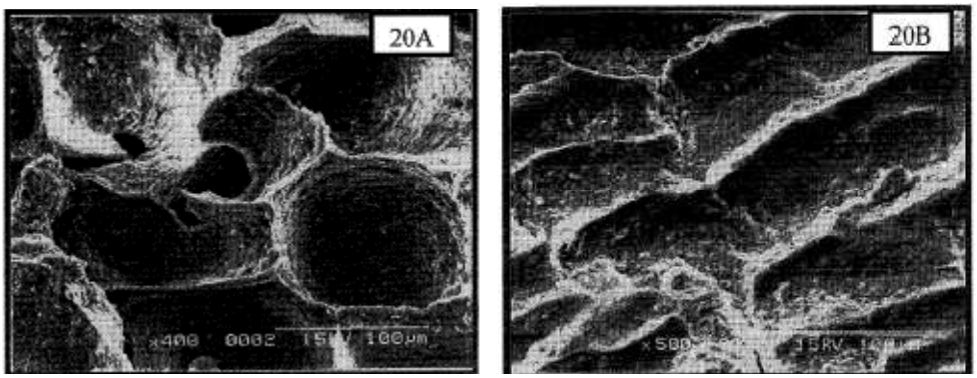

(a) (b)

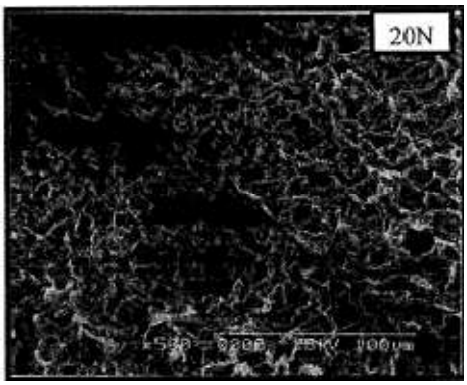

(c)

Figure 5: Kaolinite aerogels frozen at (a) -30 C (b) -50 C (c) -196 C [7]

2.2.3 Properties of Clay Aerogels

Clay aerogels are primarily characterized by both their extremely low density, ranging from 0.02 - 0.1 g•cm^{-3} for samples prepared with sodium montmorillonite, and their high porosity, in excess of 90% air by volume. Mechanically, samples of pure clay aerogels tend to be very weak and compliant, achieving compressive moduli of 14kPa-60kPa and ultimate compressive strength of 0.4 kPa to 13kPa [3] [7]. Also, a pure clay aerogel will begin to convert

back to a hydrogel in the presence of water. It would be desirable to produce aerogels that are both resistant to water and more mechanically robust. It has been shown that the addition of polymers and/or organic fibers can increase the strength of clay aerogels significantly while maintaining the same basic dry gel structure present in pure samples. The addition of 5 wt% silk fiber to a sodium montmorillonite clay aerogel was shown to increase the compressive modulus to 1.77 MPa, and further addition of 2.5 wt% PVOH increased the compressive modulus to 8.86 MPa [3]. Inclusion of thermoset epoxy precursors in the initial hydrogel, followed by elevated temperature curing, has also been shown to increase compressive strength (to 3MPa), and to allow extended contact with water without reconversion to a clay hydrogel [11].

2.2.4 Applications

Clay aerogels have shown promise in many diverse fields because of their unique properties. Due to their low solid content and small porosity they greatly reduce conduction and convection heat transfer, making them effective insulators and additives to composite cryotanks [12]. The low thermal conductivity of the clay aerogel, combined with its low density, makes them a promising replacement for foamed polymers [11]. Their high surface area makes them useful as chemical catalyst carriers and as chromatographic adsorbents [9] [13]. One unique advantage of the clay aerogel is its low environmental impact and the ease with which it can return to its natural clay state if discarded. Most possible applications hinge on the improvement of the mechanical properties and environmental stability of the clay aerogel.

2.3 Geopolymers

Geopolymers are a class of inorganic mineral polymer consisting of alkali activated aluminosilicates. Tetrahedral SiO_4 and AlO_4 are covalently linked through shared oxygen atoms into framework polymers. The bulk mechanical properties of geopolymeric binders are similar to portland cement, but with greater resistance to chemical and thermal attack. The production of geopolymeric binders also releases much less CO_2 than the production of portland cement [14]. These factors have made geopolymers of great research interest as a 'green' cement replacement. The structure and mechanical properties of the resultant geopolymeric binder are largely dependent on the molar ratio of silicon to aluminum in the material, the activator solution used, and the temperature at which the binder is cured.

2.3.1 Raw materials

Creation of a geopolymer involves two main constituents: an alkaline activating solution, and a solid source of aluminosilicates. The activator solution consists of a hydroxide donor solution in water, typically sodium hydroxide or potassium hydroxide, and an additional source of amorphous silica, typically sodium silicate, as needed to reach the desired Silica:Alumina ratio. Krivenko [15] and Davidovits [4] note that many solid aluminosilicate sources can undergo alkaline activation and form geopolymeric materials. Chief among these are natural clays (Kaolinite), dehydroxylated clays (Metakaolin), and industrial wastes (furnace slag, fly ash).

Kaolinite is one of the most widely used solid aluminosilicate sources in geopolymer research. In its raw form, kaolin can react and form a fully hardened geopolymer. However, 'metakaolin' is often used due to increased reactivity over raw kaolinite [4]. Metakaolin is kaolinite that has been dehydroxylated by kiln baking at or near 750 ^{o}C for 24 hours. This removes chemically bonded water and changes a large portion of the octahedral coordinated aluminum found in kaolin to four and five-fold configuration. Davidovits has shown that these coordinations promote greater reactivity during geopolymerization [4].

Mackenzie, et al. [16] has recently begun investigation of the suitability of the 2:1 layer clays for geopolymerization, focusing mainly on pyrophyllite. Pyrophyllite and montmorillonite are chemically similar. However, pyrophyllite is formed from metamorphic minerals such as phyllite, whereas montmorillonite is formed from the igneous feldspars. MacKenzie has shown that pyrophyllite is unsuitable for geopolymerization without significant thermo-mechanical treatment. In its raw state, the octahedral aluminum sheet of a 2:1 layer clay is protected on both sides by tetrahedral silicon sheets. This limits access of the activating solution to the aluminum, preventing dissolution and subsequent geopolymerization reactions. Thermo-mechanical processing can break up these sheets, reducing the coordination of the Al, and allowing the geopolymer reaction to take place. Montmorillonite has not been used in geopolymer research, and its potential for alkali activation is presently unknown.

Blast furnace slag and coal fly ash are both of great interest to the geopolymer research community. Blast furnace slag is a byproduct of the iron and steel industries, and coal fly ash is produced and collected in any coal burning industrial application. As industrial waste materials,

traditionally fly ash and furnace slag would simply be disposed of in a landfill. Both these materials have been shown to be very suitable for use in geopolymers. Due to the high temperatures at which they are produced, fly ash and furnace slag have significant proportions of IV and V coordinated aluminum. This results in excellent overall reactivity in the geopolymer system without the need for the additional heat treatment required to dehydroxylate the natural clays. This further reduces the overall environmental impact of the final material, and reduces costs associated with production. However, the chemical composition of these materials is dependent on the raw materials used in the original industrial application. Different coals and iron ores will have different chemical compositions, and will result in variability of the resultant fly ash or furnace slag.

2.3.2 Geopolymer Chemistry

The step-by-step reaction kinetics of the geopolymerization process are an area of relative uncertainty at present. However, with the use of in situ energy dispersive x-ray diffractometry, a significant amount of insight into the reaction process has recently been gained, and a general reaction kinetic model of the process created [17] [18]. The process by which geopolymers are created is represented by the conceptual model shown in figure 6 [14].

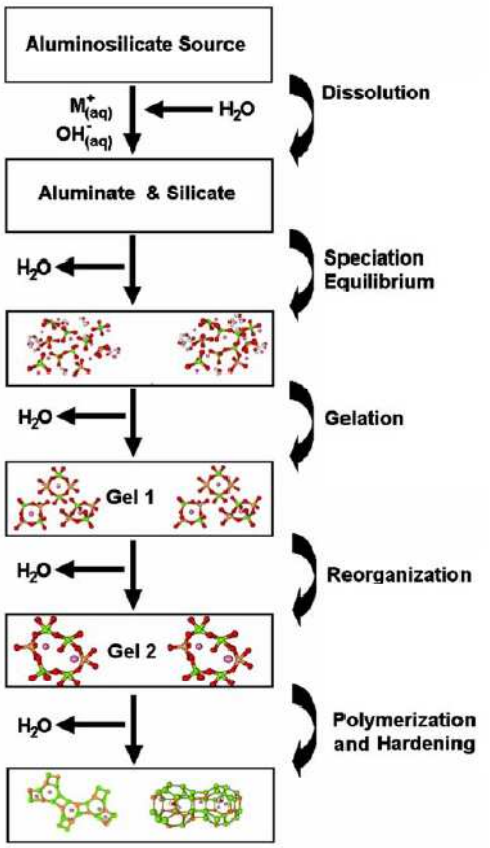

Figure 6: Schematic representation of the geopolymerization process [14]

The first step in the formation of a geopolymer is the dissolution of an aluminosilicate in the alkaline activator solution. Dissolution occurs by alkaline hydrolysis, and rapidly produces a complex mixture of aluminate and silicate species. Supersaturation by these aluminosilicate species causes precipitation and polycondensation, forming a two phase gel. This gel consists of large aluminosilicate polymer networks, with water released by the condensation reaction filling the gel pores. The reaction then enters a reorganization or 'induction' step. As time passes, areas of the gel become increasingly well-ordered, eventually forming stable nuclei which catalyze the formation of the final geopolymer network. The time required for induction can be eliminated by the addition of a small concentration of aluminum oxide seed crystals to

artificially catalyze the final polycondensation process [19]. The final structure of the geopolymer is dependent on the source of aluminosilicate and the environmental conditions under which it is cured. Curing under atmospheric conditions generally results in an amorphous structure, while elevated temperature and pressure can produce a number of zeolitic and mineral structures [4].

2.3.3 Properties of Geopolymers

Geopolymeric binders have greatly varied mechanical properties dependent on their chemical formulation. Most common geopolymer binders have properties similar to those of portland cement (Table 1). These properties vary with the composition of the binder, the activator used, and curing conditions.

Table 1: Mechanical Properties of Fly Ash Based Geopolymers [4] and Portland Cement [20]

Property	Geopolymer Binder	Portland Cement
Compressive Strength, MPa	36-83.6	57.9
Modulus of Elasticity, GPa	>2	2.92
Shrinkage on Curing	.2%-.4%	0.05%
Bulk Density, $g \bullet cm^{-3}$	1.9-2	2
Porosity	15%-30%	2.32%
Thermal Conductivity, $W \bullet (K \bullet m)^{-1}$	.2-.4	0.53

Introduction of organic polymers (such as carboxyl methyl cellulose and poly(ethylene glycol)) into the geopolymer binder can give the final cured polymer significant elasticity. Chemically, geopolymers outperform portland cements in a number of areas. The geopolymeric binder is much more resistant to acid attack, due to the protective effects of the metallic cations present in the polymer framework. This leads to less than 10%wt breakup of the geopolymer binder after 28 days in a 5% acid solution, as compared to 80-100% for the portland cement. Geopolymers have also shown greater resistance to fire and high temperatures. At temperatures greater than 400 ^{o}C, portland cement based concretes lose strength and may explode due to internal pressure from trapped water vapor. Geopolymer concrete has been shown to maintain strength greater than 20MPa at temperatures up to 1100 ^{o}C. Nano-porosity present within the geopolymer matrix allows water vapor to escape, preventing pressure build up within the matrix as the adsorbed and chemically bonded water is released [4].

Finally, geopolymeric materials have shown strong adhesive bonding with a variety of substrates, including metals, synthetic fiber reinforcement, natural stone, and portland cement concrete. This makes them good candidates for use in composite materials and in coating applications.

2.3.4 Foamed Geopolymers

Attempts have been made in the literature to produce geopolymeric materials with reduced bulk densities. Past work by E. Liefke [21] produced a low density (.1-.8 g•cm^{-3}), low thermal conductivity geopolymer foam through the addition of blowing agents like hydrogen

peroxide and sodium perborate. These blowing agents reduce the density of the foam by releasing oxygen gas during the gel phase of geopolymerization, ultimately creating large pores with 0.5 mm-3 mm diameter. This TROLIT foam has a very high application temperature (1000^{o}C) and retains good compressive strength (0.5 MPa to 2 MPa). However, pore size can be difficult to control, and careful control of the mix is required.

J. L. Bell and J. W. Kriven [22] have demonstrated the creation of geopolymer foams through the use of hydrogen peroxide or metallic aluminum powder. In alkaline environments, aluminum powder reacts with hydroxide ions and releases hydrogen gas, producing pores and reducing bulk density. The goal of these authors was the creation of a percolating network of interconnected porosities, allowing conversion of the hardened geopolymer to a ceramic without cracking due to buildup of internal steam pressure. Through the use of a constant-volume mold, these authors were able to obtain much smaller and more consistently sized pores than are produced by the TROLIT process. Using between 0.5%wt and 1.5%wt hydrogen peroxide, bulk densities between 1.23 g•cm^{-3}and 1.09 g•cm^{-3} were produced, with compressive strength greater than 49 MPa. Use of 60 %wt aluminum powder produced a foam with bulk density of 1.56 g•cm^{-3}, with an interconnected network of pores and unreported compressive strength.

2.3.5 Applications of Geopolymers

Geopolymers have shown promise in many different applications. Due to their mechanical similarity to portland cement, one of the primary applications for geopolymers is in the cement industry. Geopolymer-based concretes have been shown to perform mechanically

as well as portland cement based concretes, with the added advantages of greater chemical resistance and greater fire resistance. Environmentally, manufacture of fly ash geopolymer concrete produces about 80% less CO_2 then traditional portland cement [4]. The ability to use waste materials (fly ash, furnace slag, and mine tailings) to manufacture geopolymer concrete is also a significant advantage. Geopolymer-fiber composites have proven useful in high temperature applications. No organic polymer matrix material approaches the temperature and flame resistance seen in geopolymeric composites. Due to their strong adhesion to existing concrete and stone surfaces, geopolymer-fiber composites have shown great promise for repair and reinforcement of existing structures.

2.3.6 Fourier Transform Infrared Spectroscopy in the Study of Aluminosilicates

Infrared spectroscopy is a technique which can be used to identify and investigate the structure of chemical compounds. Molecules each have resonant frequencies at which they will vibrate, translate, or rotate. These resonant frequencies are determined by the shape of the molecule, mass of its constituent atoms, and the type and number of bonds it contains. In FTIR spectroscopy, a polychromatic infrared beam is passed through a sample of interest, exciting resonant vibrations in the sample. The beam is then passed through an interferometer, which allows application of the Fourier Transform to deconvolute the polychromatic beam into its component wavelengths. Greater amounts of IR energy are absorbed at wavelengths corresponding to the energy levels of these vibrations. Comparison with the base output of the beam allows the construction of an absorption plot and allows absorption peaks to be

identified. The intensity, location, and shape of these peaks can then be compared with data from the literature to identify the chemical compounds in the sample.

FTIR is helpful in the study of geopolymeric materials due to their generally amorphous nature, which makes interpretation of other techniques, such as x-ray diffraction, difficult. [23]. Table 2 lists common peaks associated with aluminosilicate materials.

Table 2: Characteristic vibrations of various aluminosilicate bonds [23]

wavenumber (cm^{-1})[a]	assignment[b]
950–1250 (s)	asymmetric stretching (Si–O–Si and Al–O–Si)
1165 (sh)	asymmetric stretching (Si–O–Si)
1115–1140 (sh)	asymmetric stretching (Si–O–Si and Al–O–Si)
1077 (s)	asymmetric stretching (Si–O–Si and Al–O–Si)
950–980 (sh)	Si–O stretching ($Si–O^-R^+$)
882 (s)	Si–O stretching and OH bending (Si–OH)
798 (m)	symmetric stretching (Si–O–Si)
727 (sh)	symmetric stretching (Si–O–Si and Al–O–Si)
620 (sh)	symmetric stretching (Si–O–Si and Al–O–Si)
561 (s)	symmetric stretching (Al–O–Si)
466 (s)	bending (Si–O–Si and O–Si–O)

[a] The abbreviations in parentheses are as follows: s = strong, m = medium, and sh = shoulder. [b] R = Na and K.

Rees et al. [19] [24] have extensively studied the development of the FTIR spectra of reacting fly ash geopolymers. Initially, the raw aluminosilicate source is shown to have a diffuse peak around 1000-1055 cm^{-1}. As the geopolymer reaction proceeds, this peak shifts to lower wavenumbers, and becomes more sharply defined. Rees has shown that the final geopolymer network is strongly resonant with Si-O-R stretching, which occurs from 950-980 cm^{-1}.

Chapter 3:

Experimental Work

3.1 Raw Materials

Each sample consisted of a liquid activating solution and a solid aluminosilicate source. The basic activating solution consisted of 2 parts (by weight) STARSO sodium silicate solution (PQ Corporation) and 1 Part of 10 mol•L^{-1} or 15 mol•L^{-1} NaOH solution. The NaOH solution was prepared by dissolution of NaOH pellets (reagent grade, Fisher Scientific) in tap water. The activating solution for the S+Al series also included 2 %wt dissolved sodium aluminate (Reagent grade, anhydrous, Riedel-de Haen).

Two sources of solid aluminosilicate were used in this work. S series samples were prepared using S-Type granulated furnace slag (St. Mary's Cement, Ontario, Canada), while M-series samples were prepared using Metamax metakaolin (Engelhard Corp.). Table 3 presents the chemical composition of each sample constituent.

Table 3. Chemical composition of raw materials in mass percentages.

	SiO_2	**Al_2O_3**	**Na_2O**	**K_2O**	**CaO**	**H_2O**
Metakaolin	53	43.8	0.23	0.19	0.02	--
Slag	39	7.7	0.28	0.45	39	--
Montmorillonite	68.5	17	0.65	0.15	2	--
Sodium Silicate	24	--	13.5	--	--	62.5
Sodium Aluminate	--	53	43	--	--	--

3.2 Preparation Procedure

The activating solution used for all samples was prepared by mixing the constituents in the proportions listed above. This was done immediately prior to use, as stored quantities of this activating solution were observed to form solid precipitates within 48 hours of preparation. The solid aluminosilicate source was then added to the activator solution, and blended in a high-shear, impeller-type mixer. This precursor liquid was stirred until an increase in viscosity was observed, ranging from 2 minutes to 3 hours depending on the alkalinity of the activator and reactivity of the aluminosilicate source. Once a viscosity increase was observed, samples were immediately poured into plastic molds, and allowed to mature for 24 hours. Maturation was performed under dry heat (furnace at 65 ^{o}C), moist heat (covered container over 65 ^{o}C water), and ambient conditions. Following the maturation phase, samples were deep frozen in an alcohol-dry ice bath for two hours. Finally, all samples were sublimation dried at 0.025 Torr and room temperature for 72 hours.

After drying, each sample was inspected to ensure it was acceptable for further investigation and testing. Acceptable samples appeared dry and hard, with little shrinkage in the diameter. Samples deemed unacceptable showed large surface cracks (often due to thermal shock), still appeared damp or malleable (insufficient drying), or have a sticky/foamed surface (improper maturation).

3.3 Nomenclature and Sample Composition

Samples were classified by the source of solid aluminosilicate, amount of solid added per 100g activating solution, and the presence of added sodium aluminate. Samples were named using the following nomenclature:

*a*m *b*-*c*

Where *a* indicates the molality of the NaOH solution used in the activator, *b* indicates the solid aluminosilicate source (S= S-type slag, M=metakaolin, DM=dehydroxylated montmorillonite), and *c* indicates the amount of solid aluminosilicate added (in grams) per 100g of activating solution. Samples which included added sodium aluminate have the suffix +Al. The molar ratios of reactants for each sample are listed below in Table 4.

Table 4: Molar ratios of samples

Sample	**SiO_2/Al_2O_3**	**$(Na_2O + CaO)/SiO_2$**	**$H_2O/(Na_2O + CaO)$**	**$(Na_2O + CaO)/Al_2O_3$**
15m M-5	14.41	0.97	12.03	13.98
15m M-2	32.95	1.06	12.03	34.9
10m M-5	14.41	0.85	14.21	12.25
15m S-5	79.18	1.12	10.77	89.18
15m S-5+Al	10.04	1.24	9.77	12.47
15m S-2	185.24	0.61	21.31	112.76
10m S-2	185.24	0.48	28.23	88.12
15m DM-5	7.17	0.089	6.82	0.64
15m DM-2	7.65	0.15	9.21	1.18
10m DM-5	7.17	0.083	7.59	0.59

3.4 Experimental Equipment

3.4.1 Sublimation Dryer

Sublimation drying was performed in a custom-built dryer consisting of an eight liter vacuum chamber mounted in a commercial chest freezer, a dry ice cold trap, solvent filter, and rotary vane vacuum pump (Fig 7). This system has an ultimate vacuum pressure of approximately $2x10^{-2}$ Torr and the ability to control chamber temperatures between $0^{o}C$ and $-25^{o}C$. Two thermocouples monitor chamber and freezer temperature, and a thermocouple vacuum gauge is used to monitor pressure. The cold trap is maintained at $-80\ ^{o}C$ with a dry ice/alcohol bath, and removes condensable vapors (most notably water) by freezing before they reach the pump. The corrosive filter neutralizes any NaOH which may have become volatized in the vacuum environment. This dryer allows for greater variation in sample size and geometry, at a lower cost than commercially available freeze dryers.

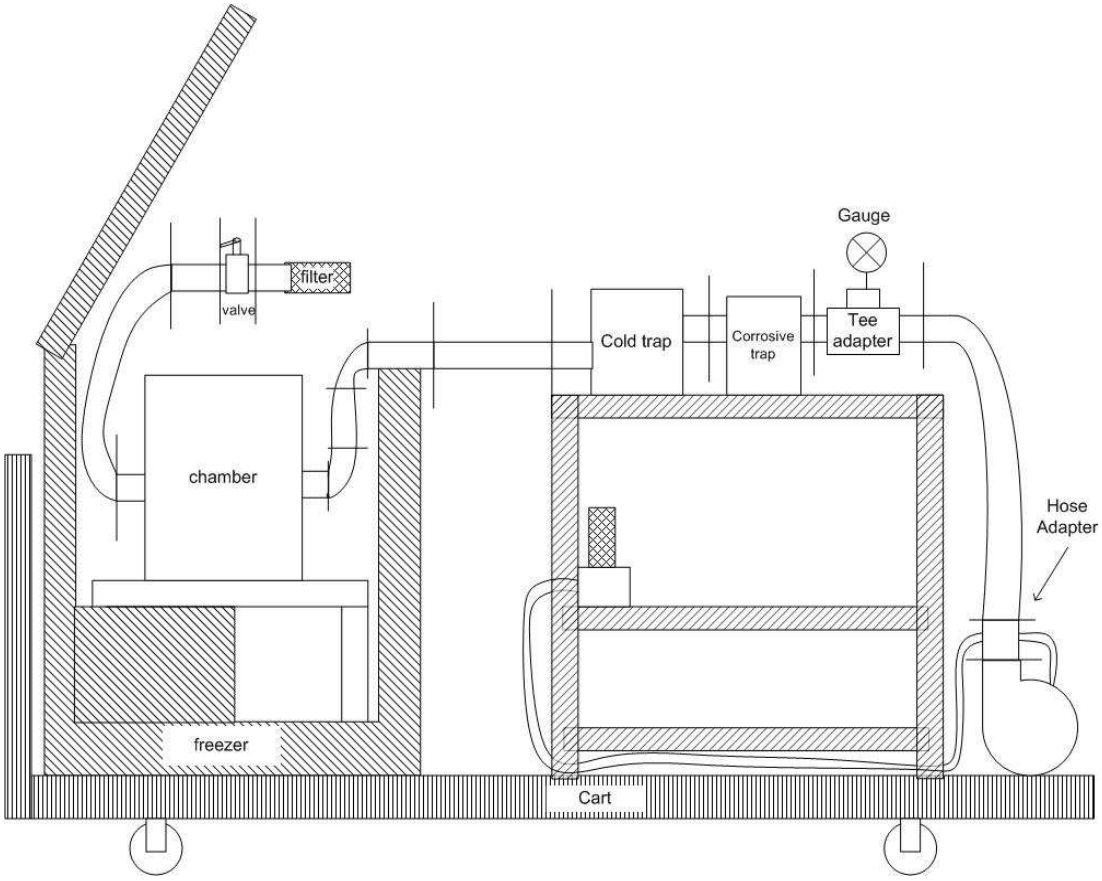

Figure 7: Sublimation dryer schematic diagram

3.4.2 Compressive Testing

The compressive strength and elastic modulus were found for all compositions using an Instron UTM, outfitted with a 1000lbf load cell and flat, circular anvils. For all tests, the crosshead displacement rate was 0.02 in•min^{-1}. Samples were one quarter of a circular disk, with nominal dimensions of 0.600" radius and 0.350" thick. Some samples required surface sanding to bring the top and bottom surfaces into parallel, or to eliminate surface irregularities.

3.4.3 Infrared Spectroscopy

FTIR was performed with a Shimadzu IR Prestige-21. IR spectra were recorded in absorbance mode, with a resolution of 4.0, and 64 scans per sample. Samples were prepared using a mortar and pestle and KBr powder (IR grade, Acros Organics). The resulting mixed powder was pressed into sample disks with a hand press for a total of approximately ten minutes prior to testing.

3.4.4 Rheology

Rheological studies were performed with a TA Instruments AR2000 rheometer, with stainless steel 40mm diameter parallel plates. Testing was performed in the flow mode with a constant applied torque of 200 microN-m, and a gap of 500 microns. Data were recorded at 0.1Hz until gellation was observed.

3.4.5 Scanning Electron Microscopy

SEM images were obtained for both uncoated and coated samples. Uncoated samples were imaged in an AMRAY 1830 up to a useful magnification of 500x. Other samples were sputter coated with a Gold Palladium alloy for high resolution images up to 2000x.

Chapter 4:

Results and Discussion

4.1 Rheology

The rheological development of all sample compositions followed the same basic pattern. Initial combination of the activator and solid aluminosilicate forms a homogeneous, relatively low viscosity mixture. As dissolution and polymerization proceed, viscosity increases until there are sufficient polymer chains of sufficient size to cause gellation. The timescale of this process depended on both the reactivity of the solid aluminosilicate, and the alkalinity of the activator solution used. The concentration of solid aluminosilicates, and the addition of sodium aluminate did not appear to affect the stir time required to achieve gellation. Stir times to gellation are tabulated below in Table 5.

Table 5: Approximate stir time required to produce thickening

Sample	Approx. Stir Time to Thickening (min)	Notes
15m M-5	35	
15m M-2	35	
10m M-5	185	Forms weak gel, often with phase separation
15m S-5	5	
15m S-2	5	
15m S-5+Al	5	
10m S-5	140	Forms weak gel
15m DM-5	20	
15m DM-2	20	
10m DM-5	90	Forms weak gel, often with phase separation

This change in viscosity was also explored quantitatively using a rheometer. Figures 8 and 9 show the increase in viscosity with time as the polymerization reaction proceeds. Initially the viscosity changes slowly, as the solid aluminosilicate dissolves into the activating solution.

This creates a complex mixture of low molecular weight aluminate and silicate species. As the solution becomes super saturated by these molecules, they begin to precipitate out of solution and condense into larger molecules, increasing the observed viscosity. With the passage of time these molecules form 3D networks of increasing size, eventually coalescing into a rigid gel and causing the slope of viscosity with time to approach infinity.

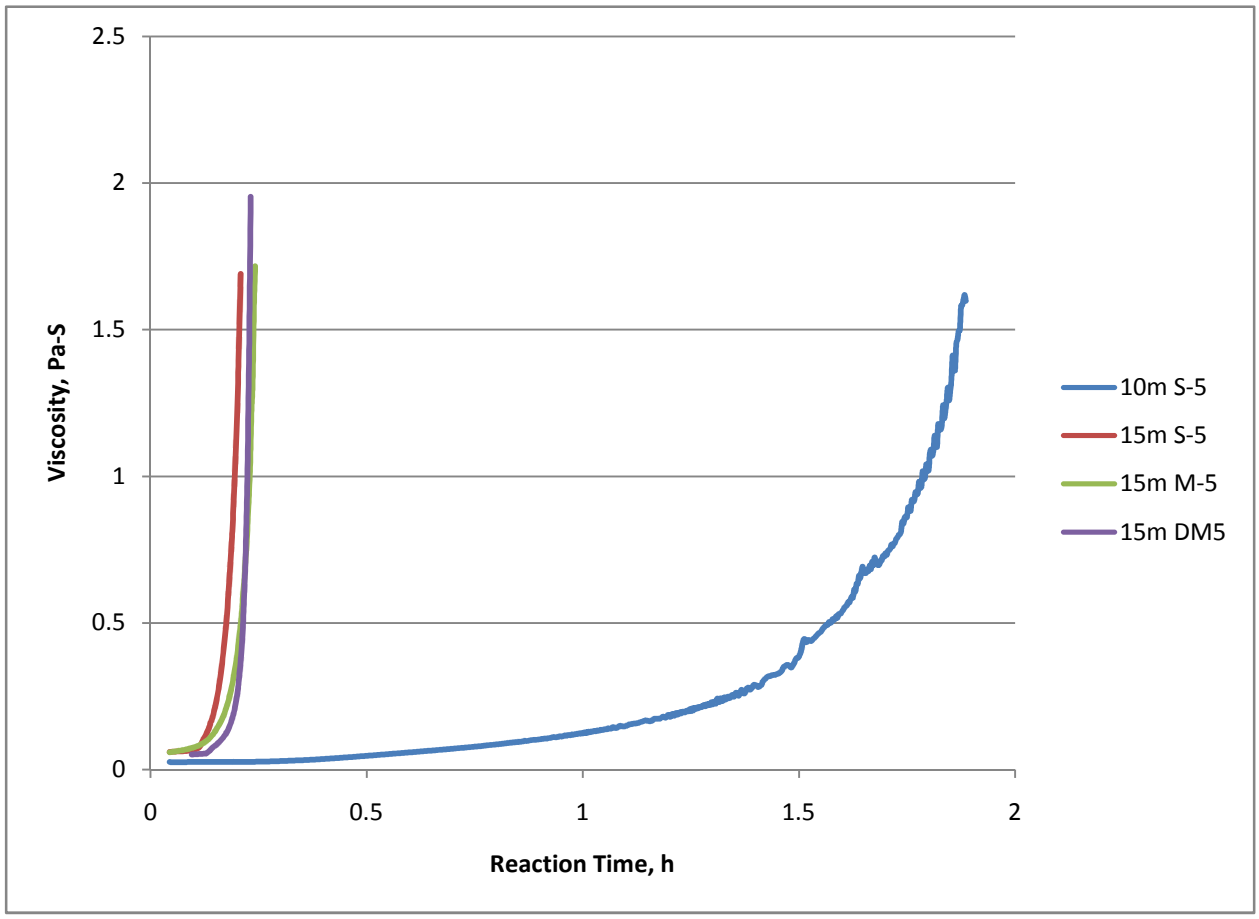

Figure 8: Viscosity as a function of reaction time for selected sample compositions.

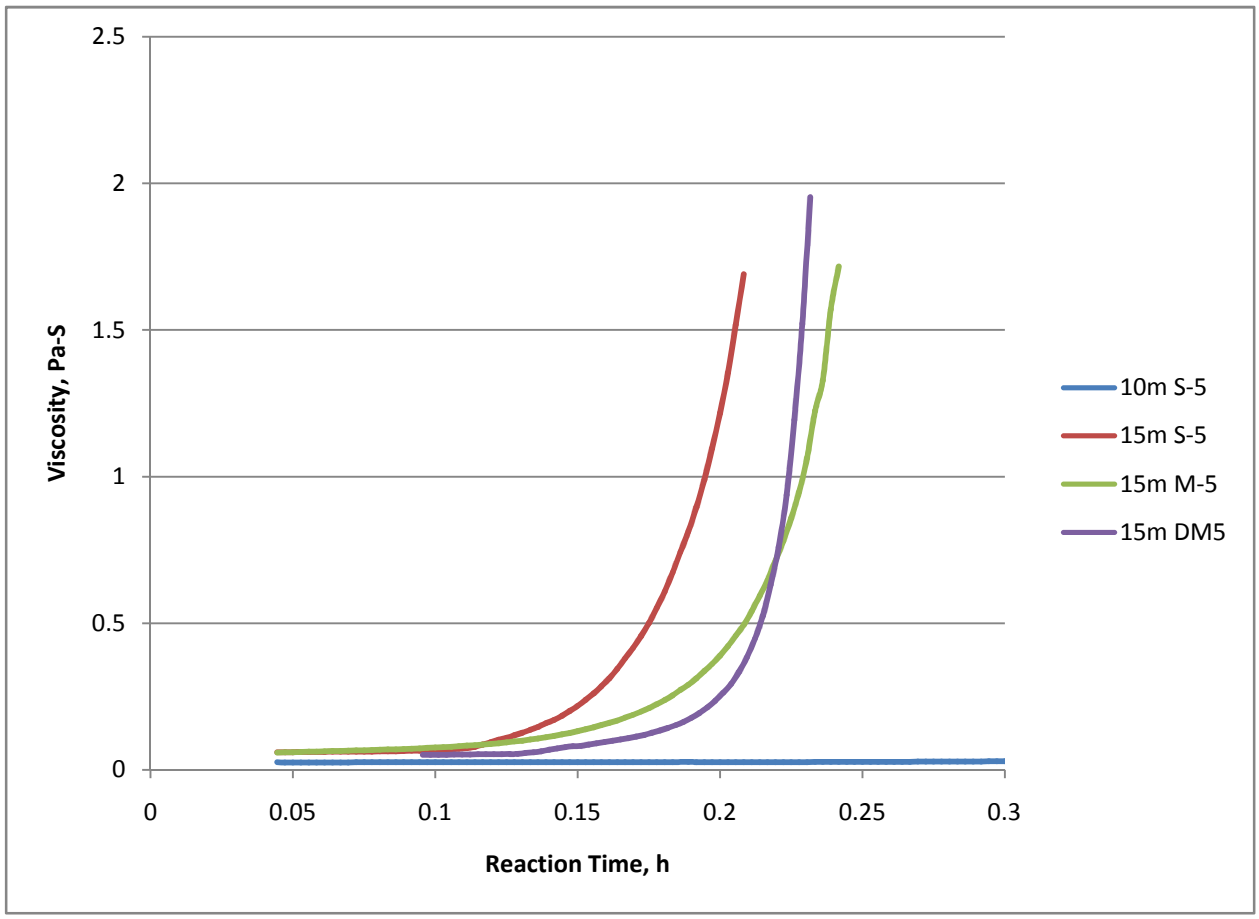

Figure 9: Detail of Figure 8

The data show that both the dissolution and polymerization steps of the geopolymer reaction proceed much faster with the use of the 15m activating solution. Samples made with the 10m activating solution required much greater stir times to show an increase in viscosity. Even when sufficiently increased stir times were used, the 10m samples formed a much weaker, more translucent gel than similar samples made with the 15m activator. When allowed to mature, these weaker gels would become biphasic, with the semi-solid gel rejecting a supernatant liquid. This seems to indicate the geopolymer reaction is unable to proceed to completion in the 10m samples.

4.2 Effect of Maturation Conditions

In the early stages of the project, several different maturation conditions were investigated for the 15m S-5 series samples. Initially, it was thought that maturation at elevated temperature would allow more complete reaction of the slag and silicates, creating a more cross linked and therefore stronger final material. Maturation of the gel was initially attempted at 65^{o}C in both low humidity and high humidity environments. In practice, samples matured at elevated temperatures became inhomogeneous; unreacted aluminosilicate particles readily precipitate out of the activator solution, creating two separate phases. This phase separation was observed in both low and high humidity environments. Attempts to sublimation dry these phase-separated samples produce a putty-like solid, sticky with unreacted alkaline silicate solution. The lack of pores in this alkaline silicate coating inhibits removal of water vapor during the drying process, often producing a foaming effect, as seen in Figure 10. Samples matured at room temperature produced a single macroscopic phase, a rigid, semi-solid gel (Fig 11).

Figure 10: 15m S-5 sample, matured at 65 ^{o}C under humid conditions.

Figure 11: Fully gelled sample, matured under ambient conditions

4.3 FTIR Analysis

All well-reacted samples showed similar changes in their FTIR spectra. Previous research by Lee and van Deventer [23] and Rees et al. [24] [25], have shown there are 2 main attenuation bands of interest in alkali activated materials. The first band, from 630-760 cm^{-1}, is associated with aluminosilicate ring and cage structures, and the second, from 800-1200 cm^{-1}, is known as the geopolymer 'main band' and is associated with asymmetric stretching of Si-O-T bonds, where T is a metallic ion such as Al. Also of interest to this discussion, due to the very high Silica:Alumina ratios used in these samples, is the band near 460 cm^{-1}, which is associated with the bending of Si-O-Si bonds.

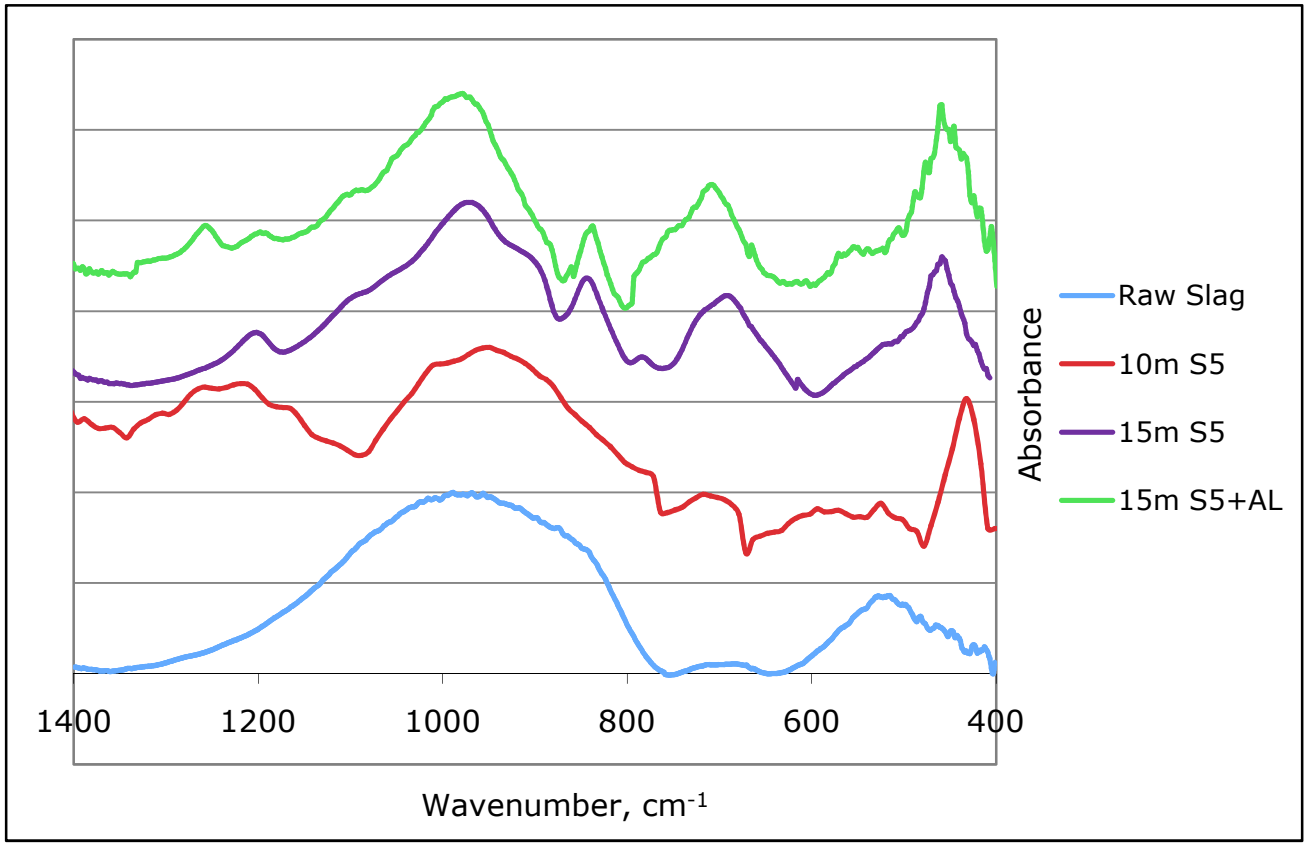

Figure 12: FTIR Spectra for slag samples

FTIR Spectra for selected slag samples are presented in Figure 12. The spectrum for raw slag displays a broad hump centered about 1010 cm^{-1}, representative of the presence of many disorganized species of aluminosilicates. There is little absorbance in the 630-760 cm^{-1} band, indicating there are few of the more complex polymeric ring and cage structures. All samples show the development of a new peak near 450 cm^{-1}, which is consistent with the addition of silicates from the activating solution. Both the 15m S5 and 15m S5+Al samples show significant changes from the raw slag. The diffuse hump in the main geopolymer band became sharper, and shifted to lower wavenumbers (990 cm^{-1} for the 15m S5+Al and 977 cm^{-1} for the 15m S5). Lee and van Deventer suggest that this shift in the Si-O-T should be circumscribed to the alkali activation process, with larger shifts indicating a higher degree of activation [23]. Both these samples also show the development of a new peak between 630 and 790 cm^{-1}, which is consistent with the development of a significant number of ring and cage polymeric structures within these samples. The sample activated with the 10m activating solution showed little change to the broad main band observed in the raw slag, and only limited development of the ring and cage polymer band. This is in agreement with observations that the 10m samples failed to fully react, producing a wet pliable material.

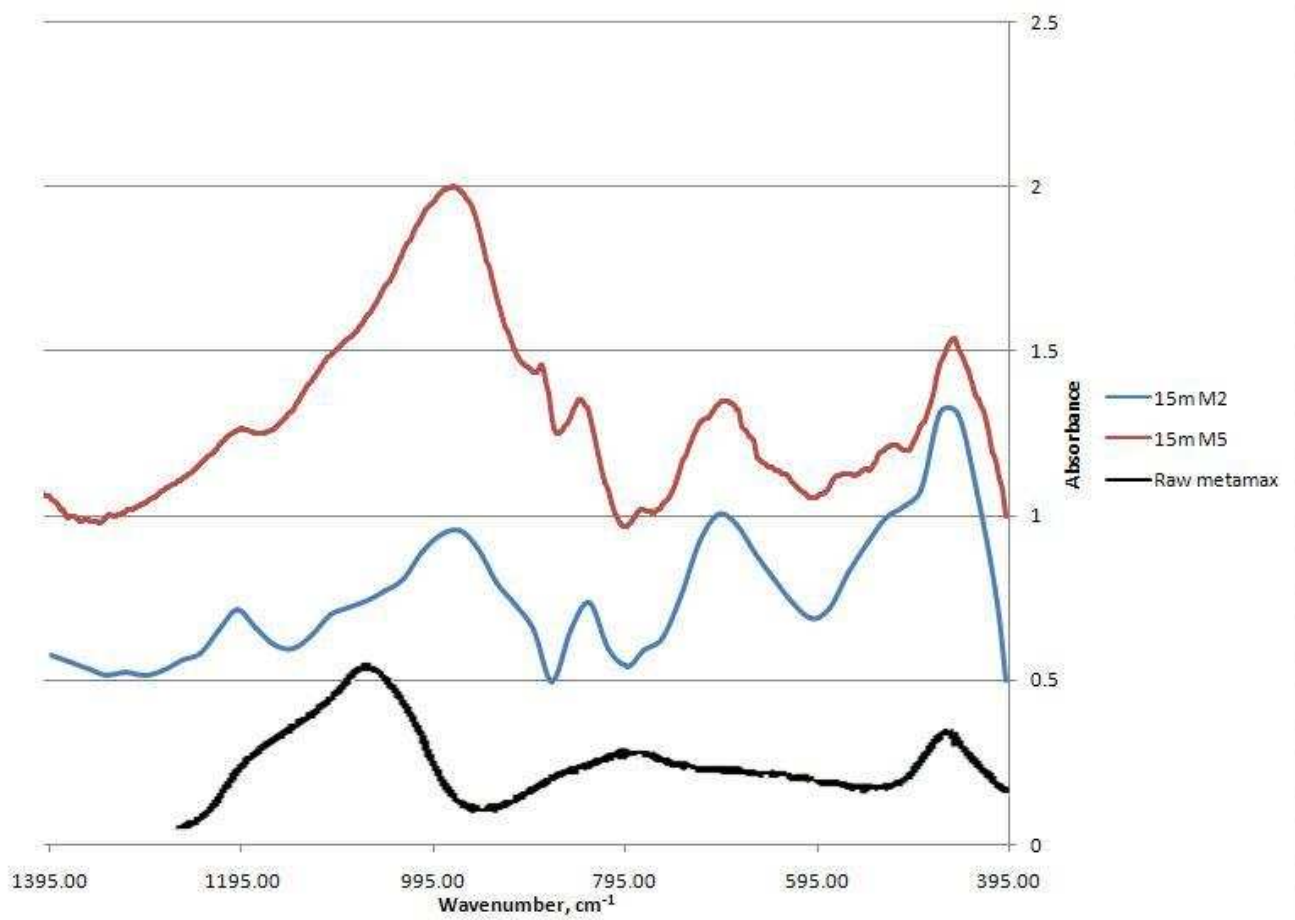

Figure 13: Spectra for Metamax samples. Raw Metamax spectra from Heller-Kallai [26]

The FTIR spectra for selected Metamax samples are presented in Figure 13. The raw Metamax displays a broad peak from ~1200-1000 cm^{-1}, centered about 1050 cm^{-1}. Both the 15m M2 and 15m M5 samples display a shift of this peak to lower wavenumbers, about 965 cm^{-1}. The main difference of interest is in the relative size and shape of this main band. The M5 has greater amount of solid aluminosilicate, and thus a reduced Silica:Alumina ratio over the M2 sample (14.4 vs. 33.0). This increase in available aluminum, has allowed the creation of a greater number of Si-O-T bonds and thus a larger, more defined peak in the main band for the

M5 sample. These samples also display the silicate peak centered about 447 cm^{-1}, and the development of the polymeric ring and cage vibrations centered about 685 cm^{-1}.

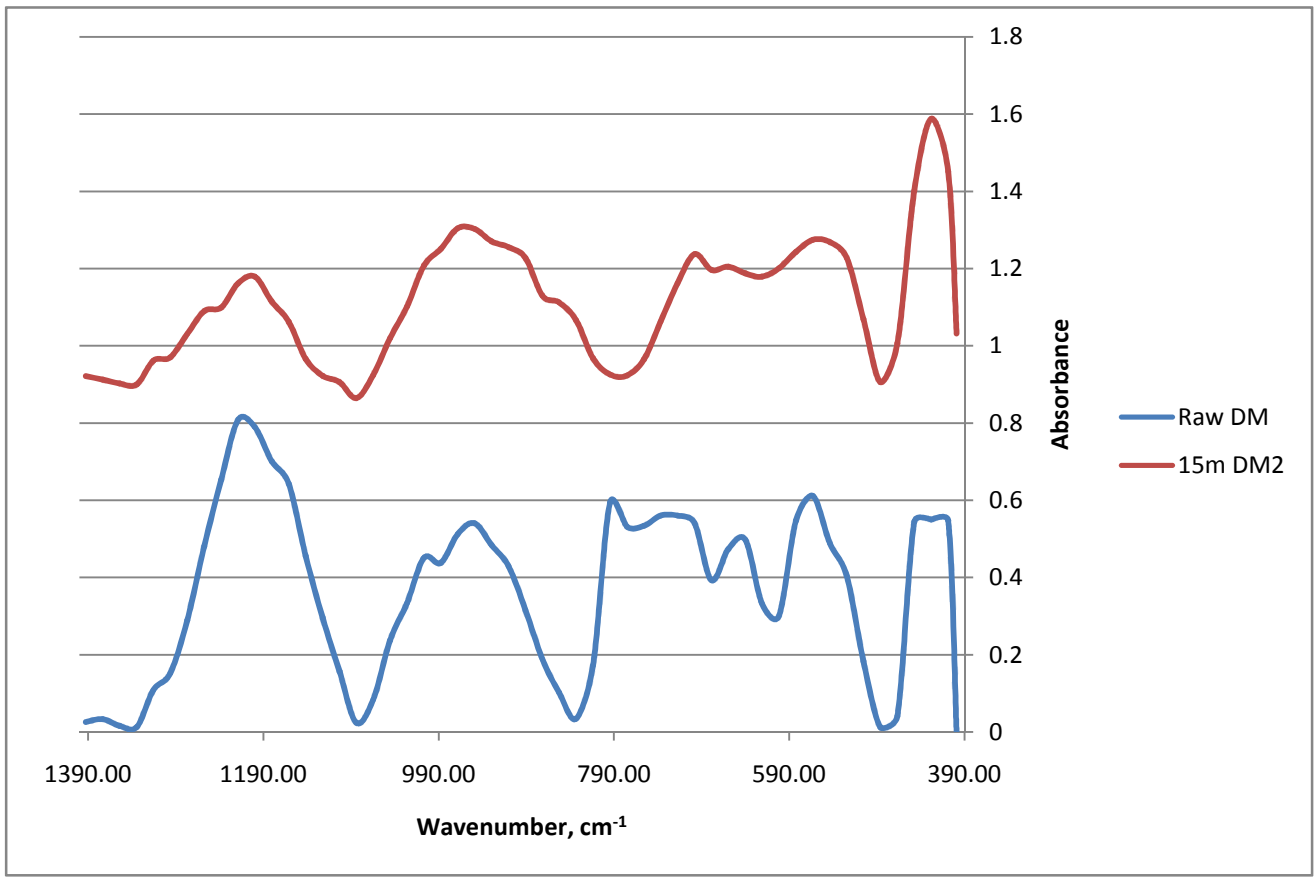

Figure 14: FTIR spectra for dehydroxylated montmorillonite samples

The spectra presented for the raw dehydroxylated montmorillonite and the reacted sample 15m DM5 are very similar. The main band peak in both the raw and reacted samples are both centered about 949 cm^{-1} indicating little alkali activation has occurred. Even in the raw material, this peak is relatively sharp, possibly indicating the presence of significant amounts of crystalline phase aluminosilicates [23], which have been shown to react much less readily then the glassy aluminosilicates [4]. A group of sharp peaks from 500-800 cm^{-1} is also

observed in both samples, possibly indicating the presence of more complex and relatively unreactive structures present in the raw material.

4.4 Compressive Strength and Elastic Modulus

Discussion of mechanical properties is limited to the samples synthesized with 15m activating solution. In the 10m samples the geopolymerization reaction is observed to proceed 9 to 10 times more slowly than similar 15m samples. This greatly reduces the amount of geopolymer formed over the 7 day test cycle used in this study, and results in samples' universally poor mechanical strength and moduli. With greatly increased reaction time, it is possible that the material could reach an acceptable level of strength, but such an increase would be impractical in most applications and was not investigated.

Average compressive strength and modulus of the dried material were dependant on both sample composition and final density. Samples which were selected for compressive testing had few surface cracks, and appeared dry and hard. Sample density was also considered, and those deviating strongly from the average were not tested. Average results for density, elastic modulus and compressive strength are presented below in Table 6. All average mechanical properties were determined based on six separate samples in each series, the stress-strain curves for which are shown in Figures 18-24.

Table 6: Average mechanical properties

Sample	Average Compressive Strength (MPa)	Average Elastic Modulus (MPa)	Average Density ($g \bullet cm^{-3}$)
15m M-5	3.572	72.23	0.912
15m M-2	0.777	118.16	0.948
15m S-5	5.093	373.13	1.249
15m S-2	4.672	116.29	0.820
15m S-5+Al	9.935	217.87	1.029
15m DM-5	2.208	85.68	0.818
15m DM-2	3.664	100.3	0.813

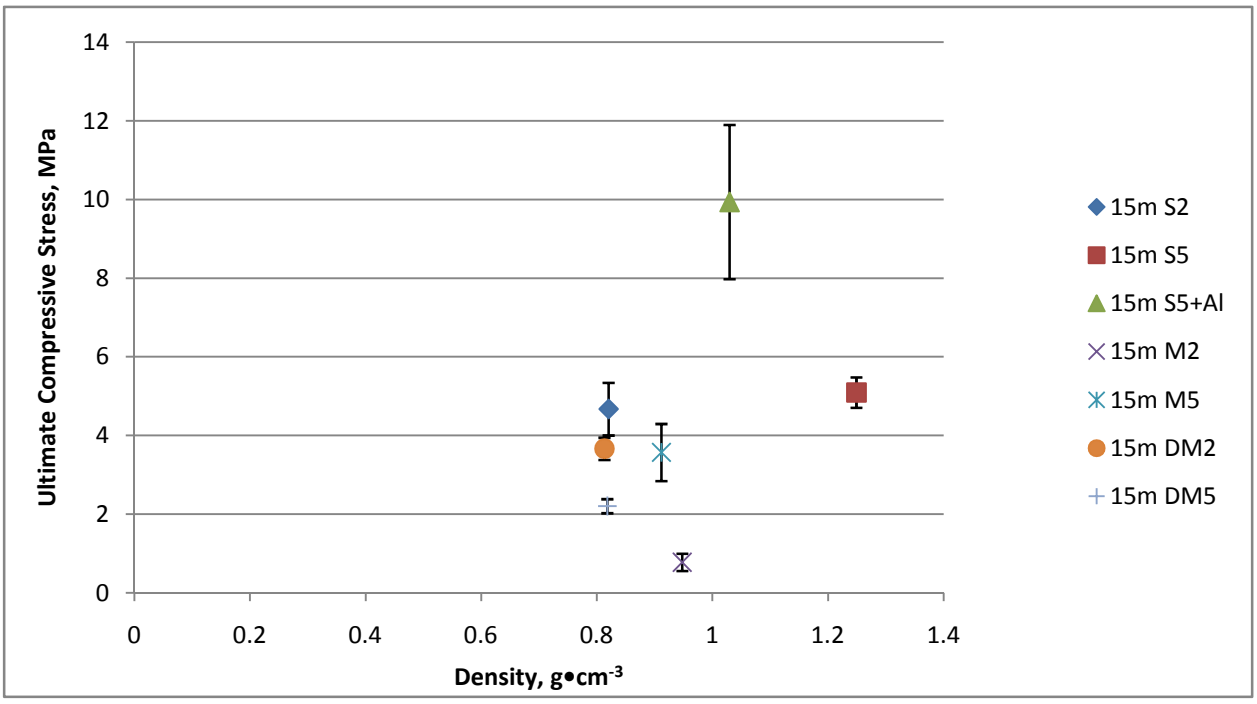

Figure 15: Average Compressive Strength and density, with 1 σ error bars.

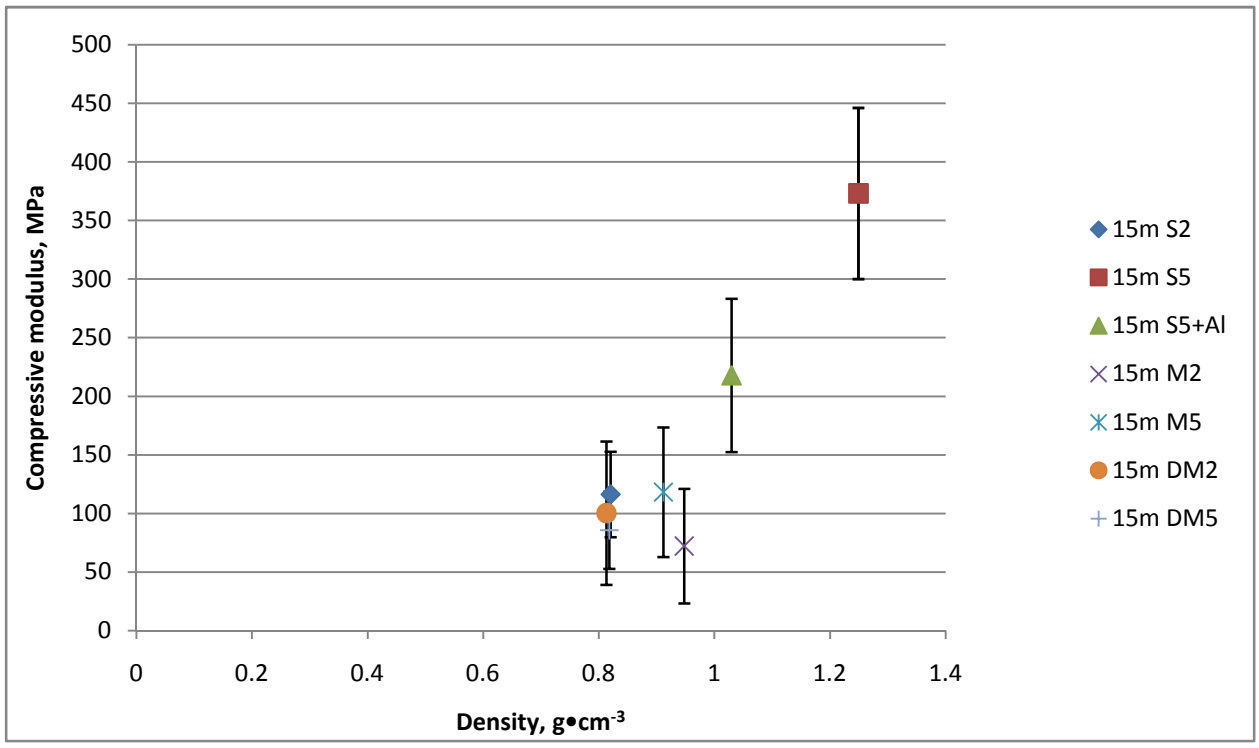

Figure 16: Elastic modulus results with 1 σ error bars.

4.4.1 Effects of Density

Changes in final density, depending on their cause, were observed to have opposite effects on the mechanical properties of the alkali activated aerogels. Two main variables in the density of this material are the porosity within the geopolymer network, and the amount of water removed by the freeze drying process. The amount and distribution of porosity is believed to be determined by the initial chemical composition of the sample, and stir/maturation procedures, and so is considered constant for each sample series. Holding water content constant, an increase in porosity will result in a reduced bulk density. Increased porosity also implies a less well connected microstructure, which explains the observed proportionality between density and elastic modulus presented in Figure 16. Density variations

observed within each sample series are believed to stem from variation in the amount of water removed by the freeze drying process. More dense samples retain greater amounts of water, and are observed to behave more like the wet-gel precursor than the stronger and more brittle fully dried material. Within each sample series, compressive strength and elastic modulus are inversely proportional to density. Figure 17 presents this effect for the 15m M-5 series.

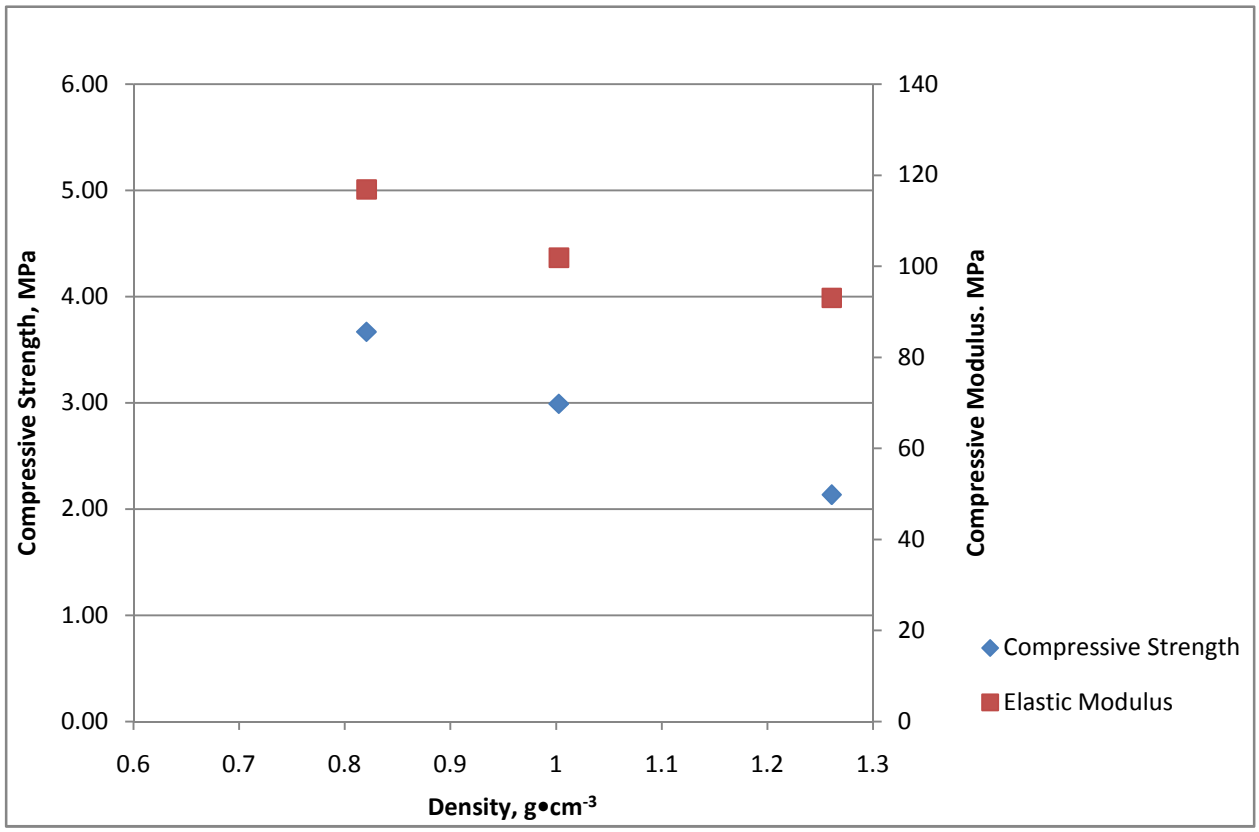

Figure 17: Average mechanical properties of 15m M-5 samples with variation in density

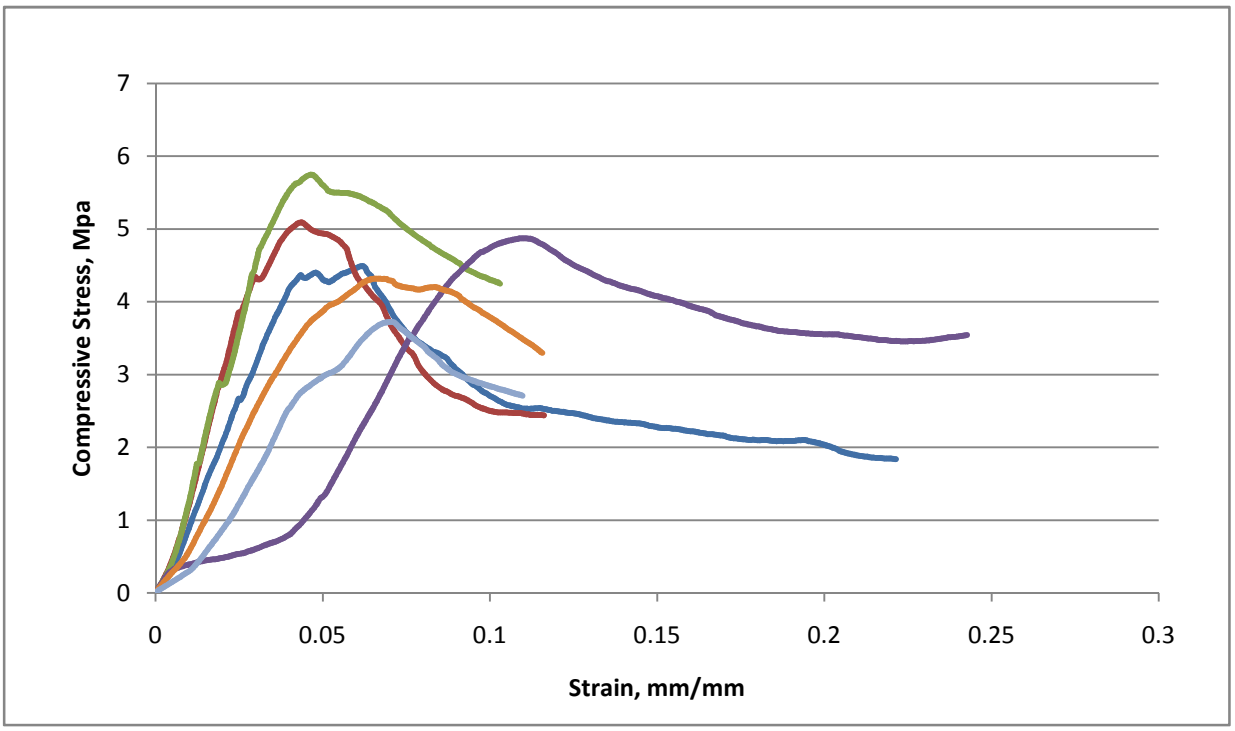

Figure 18: Stress v. Strain curve for all 15m S2 samples

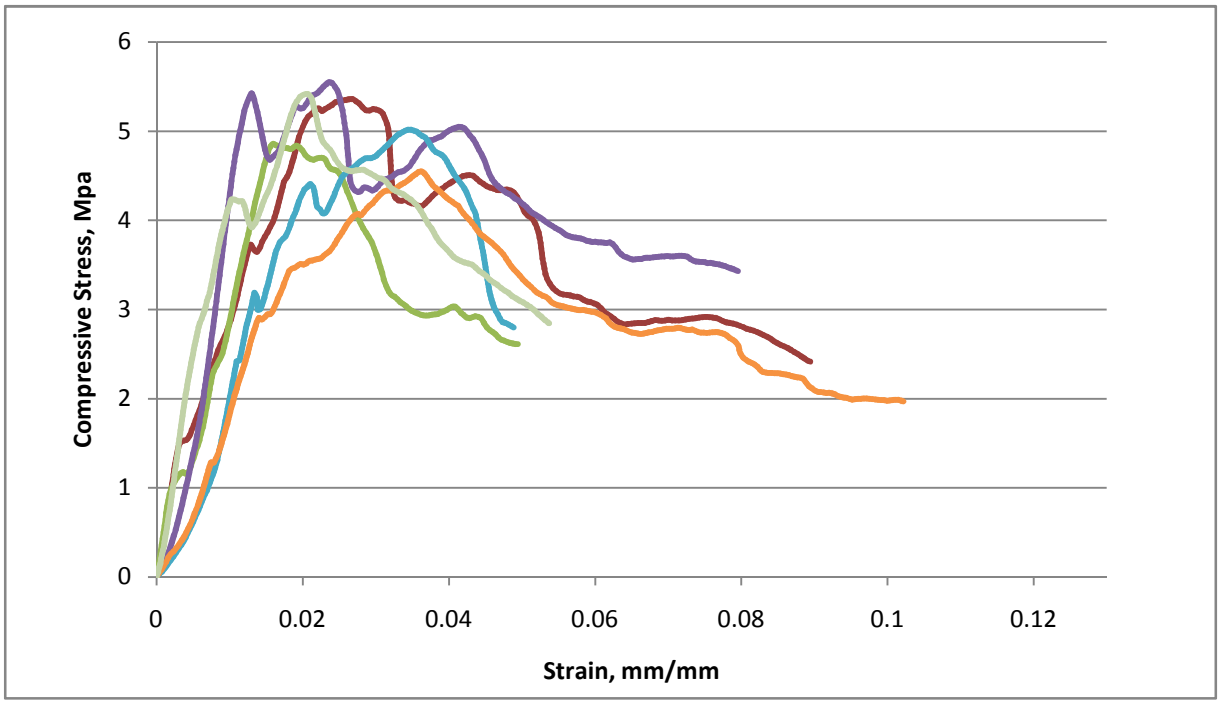

Figure 19: Stress v. Strain curves for all 15m S5 samples

Stress-strain curves for the 15m S5 and S2 samples are presented above in Figures 18 &19. Both plain slag compositions have similar average compressive strengths. However, the 15m S2 samples had significantly lower densities and elastic moduli. Both these changes can be attributed to the reduction of available solid aluminosilicate as a reactant. This produces a less well-connected geopolymer network, with fewer Si-O-Al bonds. The final material has greater porosity and thus reduced density and elastic modulus.

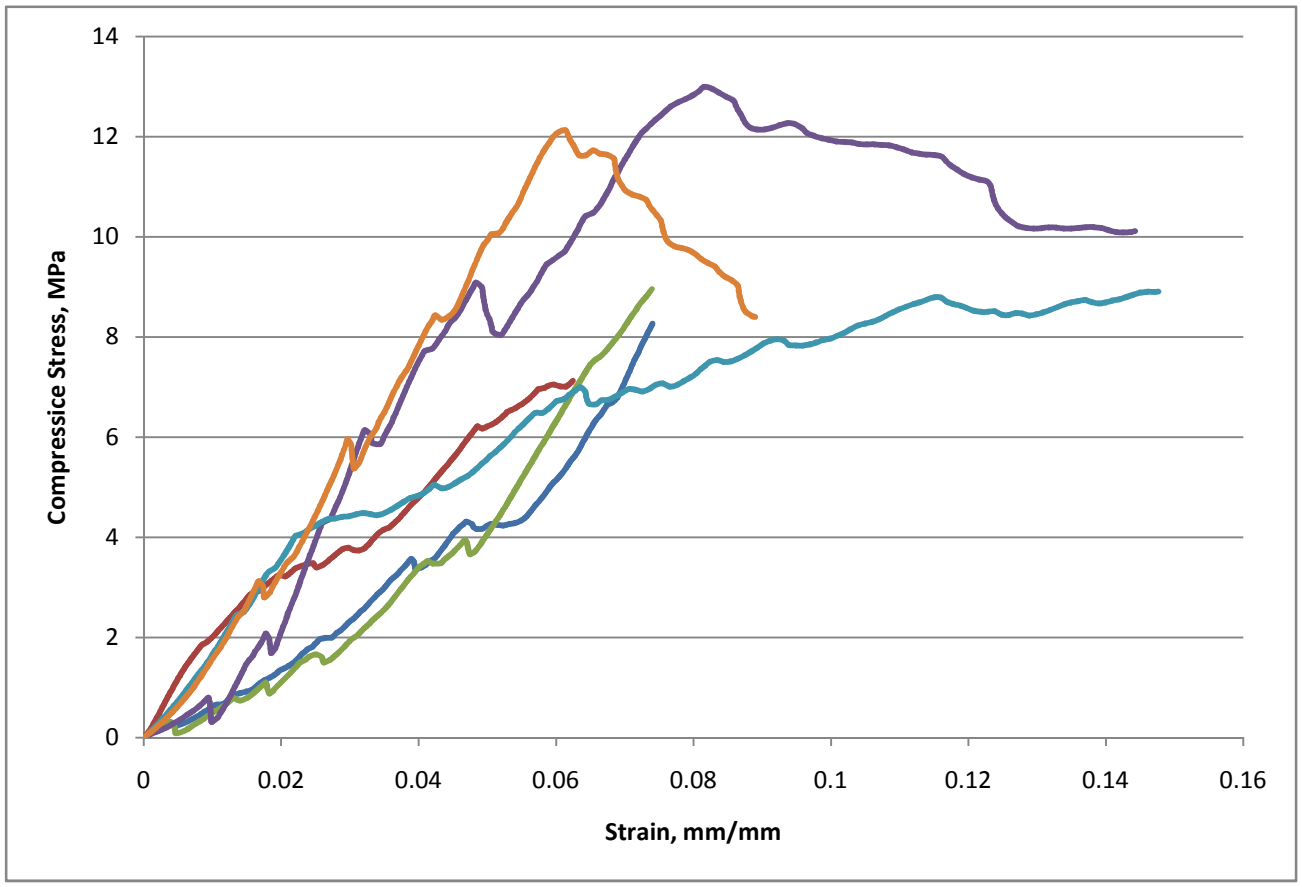

Figure 20: Stress v. strain curves for all 15m S5+Al samples

Stress-strain curves for the 15m S5+Al samples are presented in Figure 20. The addition of sodium aluminate nearly doubled the compressive strength of the 15m S5+al samples over

that of the 15m S5 samples. Sodium aluminate is a very good source of aluminum metal ions when dissolved in solution, and brings the molar Silica:Alumina ratio of these samples down to 10. This addition of aluminum ions allows more Al-O-Al and Al-O-Si bonds to form, creating a stronger final material. While compressive strength was improved, both the density and elastic modulus of these samples was reduced.

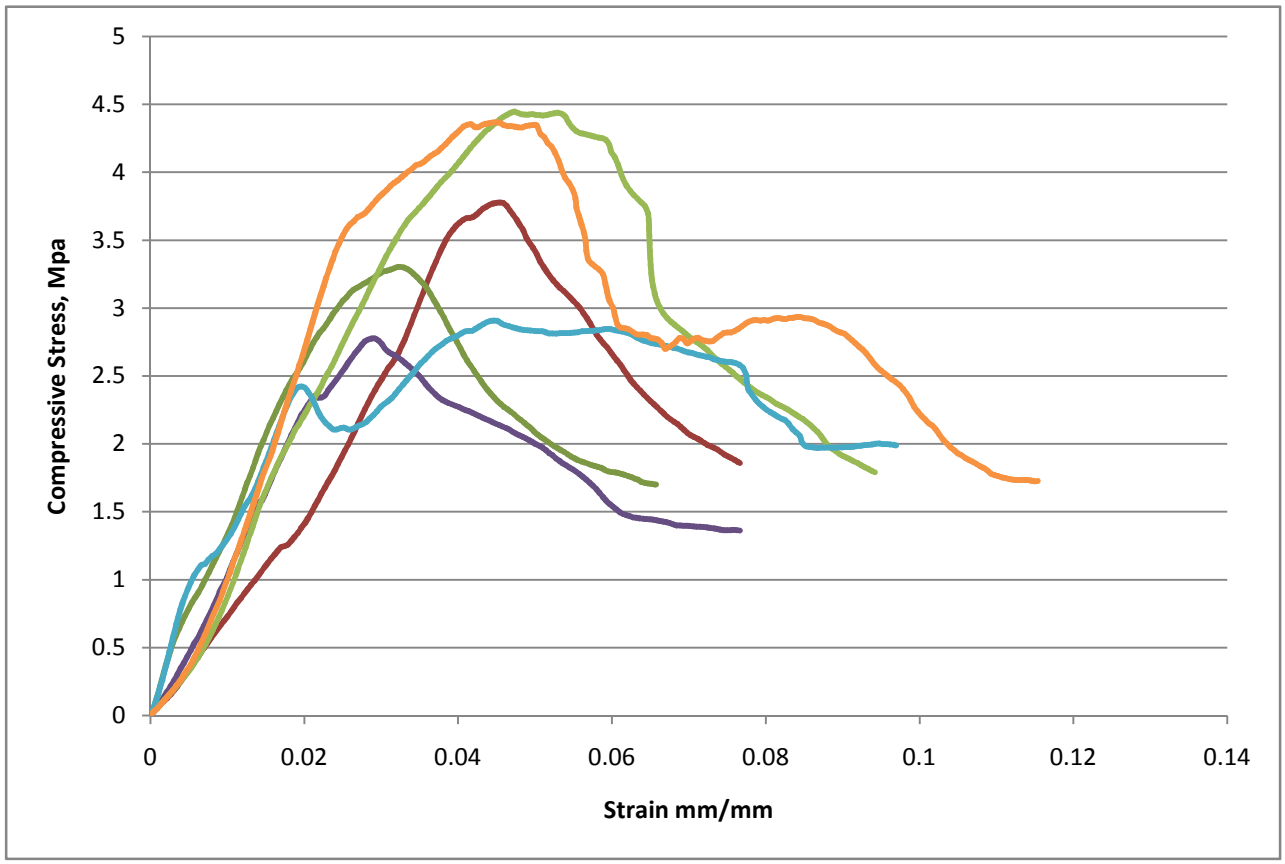

Figure 21: Stress v. Strain curves for all 15m M5 samples

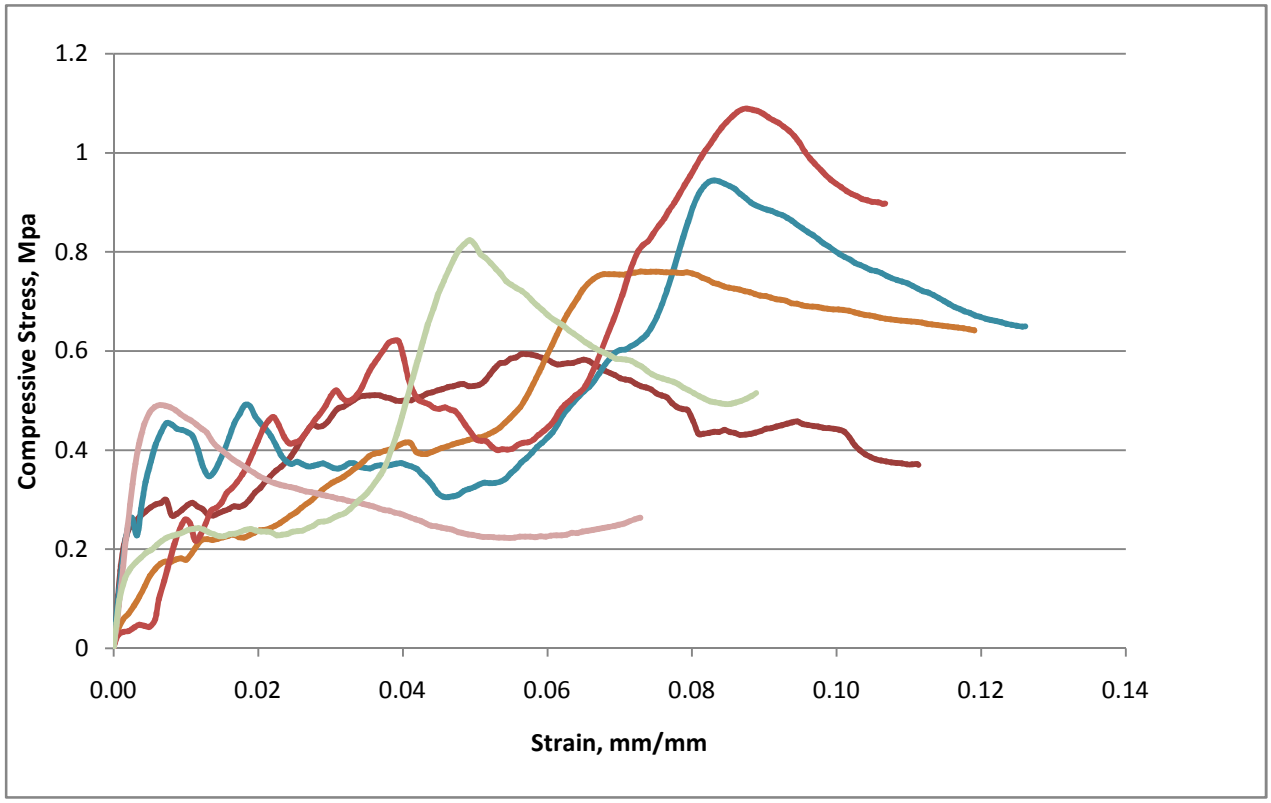

Figure 22: Stress v strain curves for all 15m M2 samples.

Both the 15m M5 and M2 samples displayed greatly reduced compressive strengths and moduli relative to similar slag samples. The longer observed reaction times required to produce gellation in these samples indicates that the Metamax is generally less reactive than the slag under these conditions. Since the reaction proceeds more slowly, it is likely that a smaller proportion of the available aluminosilicate is geopolymerized in these samples. This produces a less well-connected polymer network, and therefore a mechanically weaker material.

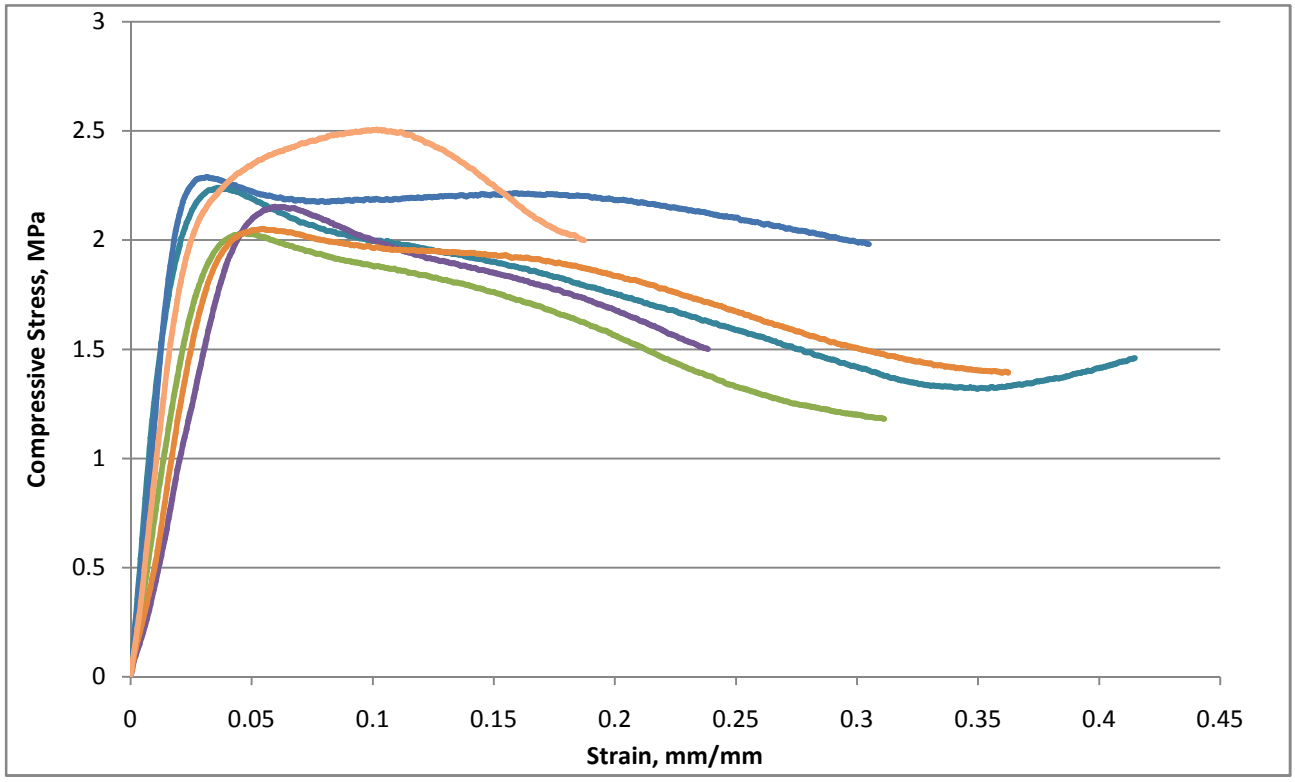

Figure 23: Stress v. Strain curves for all 15m DM5 samples

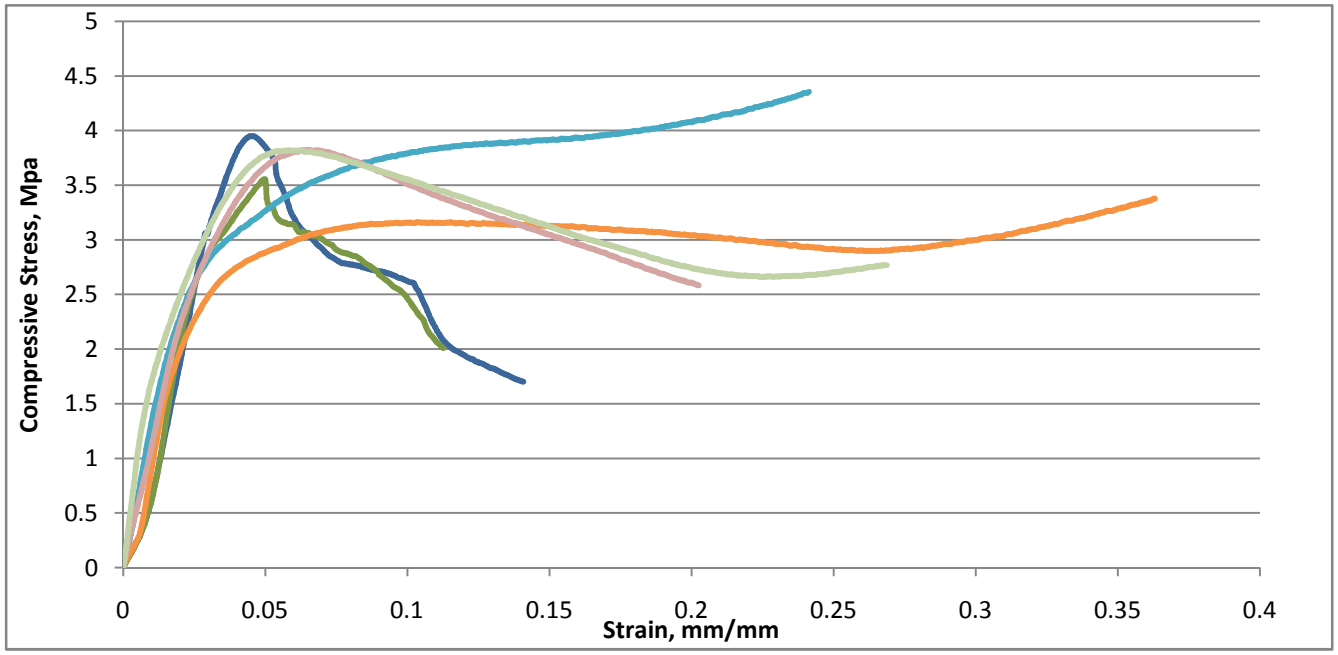

Figure 24: Stress v. strain curves for all 15m DM2 samples

Results for the Dehydroxylated Montmorillonite samples were quite similar to the samples made with Metamax. The montmorillonite also displayed slower reaction times than similar slag samples, leading to reduced overall geopolymerization and mechanical strength.

Of the three solid aluminosilicates investigated, the furnace slag seems to have the greatest overall reactivity and consequently the best mechanical properties. Both the metakaolin and dehydroxylated montmorillonite share similarly reduced reactivity and mechanical properties relative to the furnace slag. From the average results, it appears that the compressive modulus for these materials is proportional to density. As density is reduced, a greater proportion of the material is comprised of air-filled pores. Logically, this more open structure should (and does) result in a reduction in compressive modulus.

4.5 Scanning Electron Microscopy

Figures 25 and 26 present SEM images of a 15m furnace slag, and 15m Metakaolin sample, respectively. Both these samples exhibited very similar microstructures. In the interior, large number of pores approximately 20-30 microns in diameter can be observed. In the wet gel state, these pores were filled with a liquid solution composed largely of water, unreacted silicate and aluminate species, sodium ions, and hydroxide ions. This water was removed during the freeze drying process without collapsing the surrounding polymer network, leaving an air filled pore. On the surface very few of these pores are observed. During the ambient maturation process, water was able to evaporate from the sample. Surface tension and capillary forces during evaporation collapse the porous gel network, leaving the closed solid network seen in Figure 25 (b). The evaporation of water at the surface also results in ion

migration, creating a white deposit of salts on the sample surface. It is believed that this more rigid surface coating may hinder the removal of water during the freeze drying process; making it difficult to obtain a fully dry material.

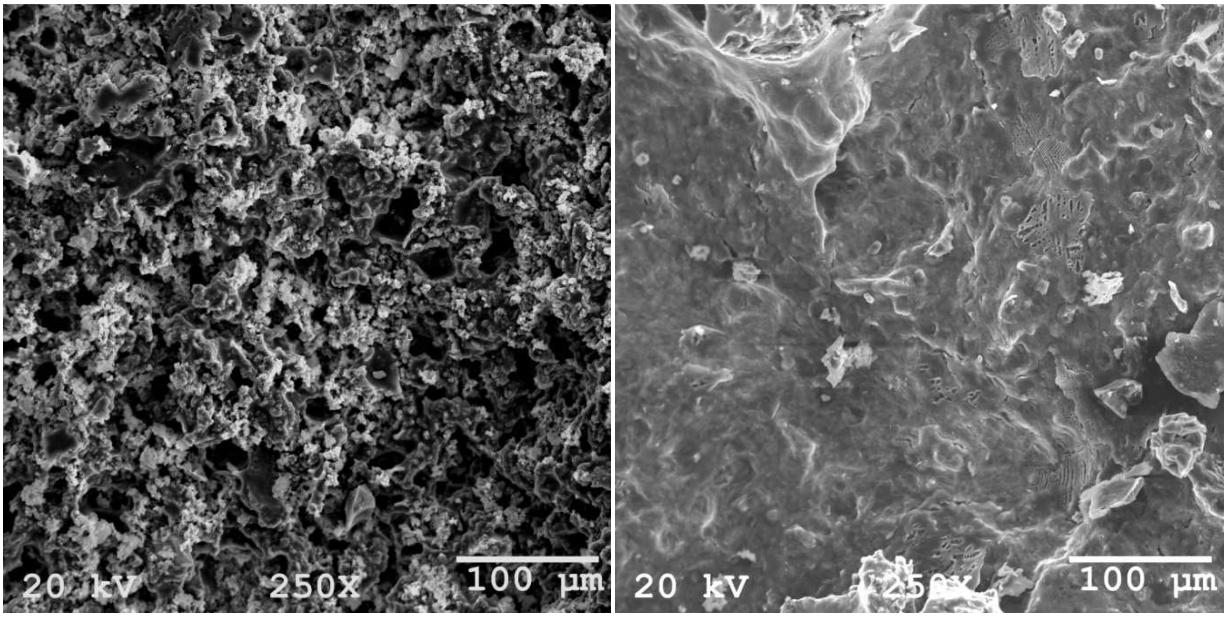

(a) (b)

Figure 25: SEM image of 15m S5 sample at 250x magnification (a)Sample interior (b) Sample surface

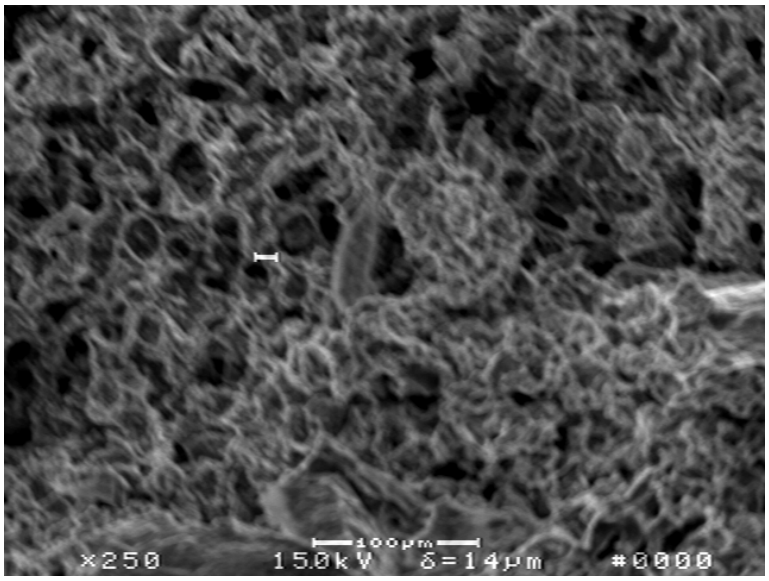

Figure 26: SEM image of 15m M5 sample at 250x magnification (interior)

Figure 27 shows the same furnace slag sample at higher magnification. Among the glassy polymer network more regular, sharp deposits can be observed in many areas. We suspect these deposits represent solutes present in the pores of the wet gel which cannot be removed by the freeze drying process, especially sodium and calcium formations.

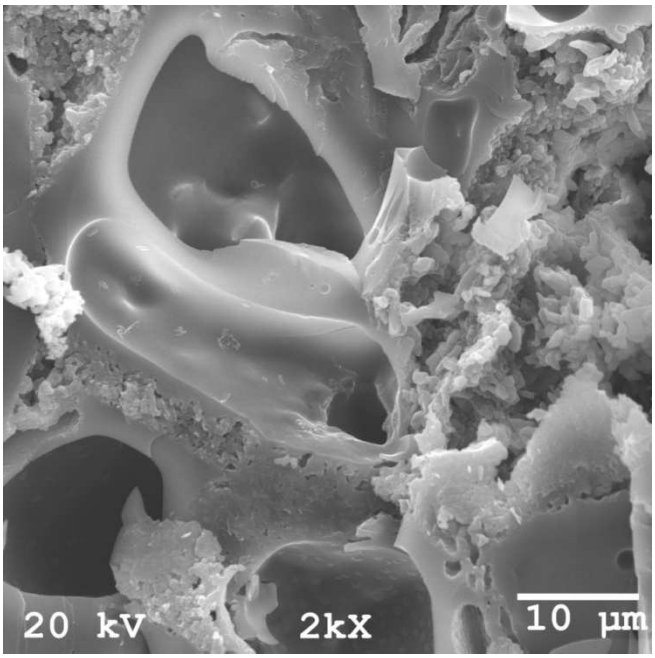

Figure 27: SEM image of 15m S5 sample at 2000x magnification (interior)

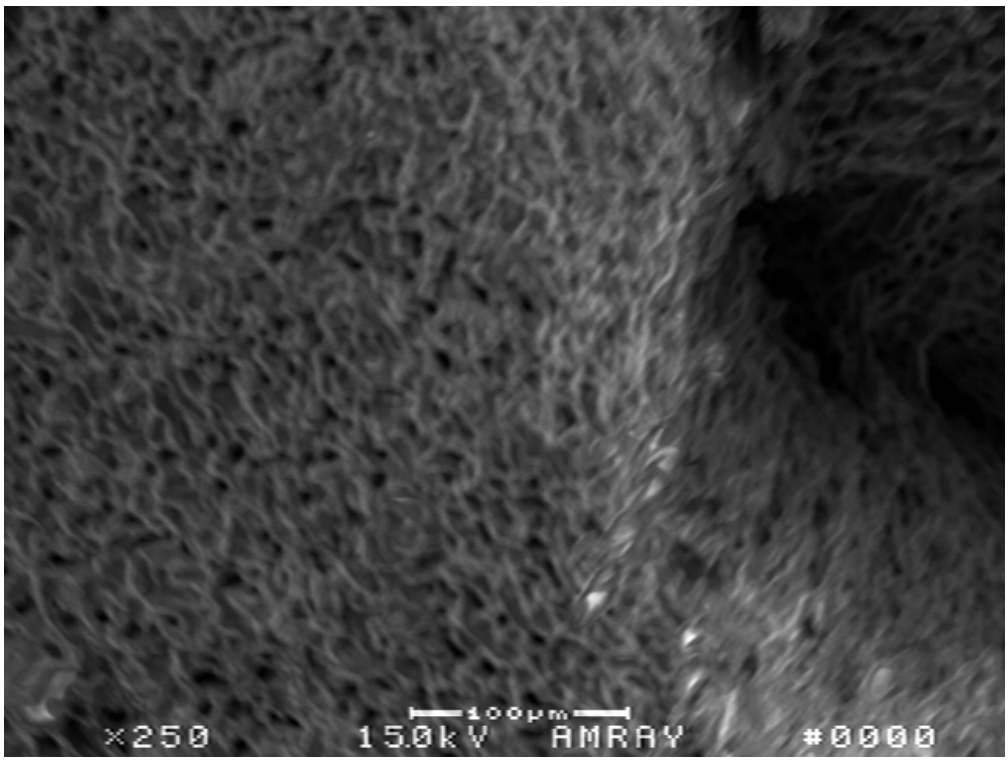

Figure 28: SEM image of 15m S5+Al sample at 250x magnification (interior)

The addition of sodium aluminate had a strong influence on the observed microstructure of the slag samples. Pore size is reduced to approximately 10 microns, and pores are much more regularly sized. The overall appearance of the polymer network is much more orderly and regular than any of the other samples. As mentioned earlier, the addition of aluminum ions allows the geopolymer reaction to proceed more completely, allowing increased polymerization and crosslinking of the available aluminosilicates. This results in the more regular, tightly knit structure observed in Figure 28.

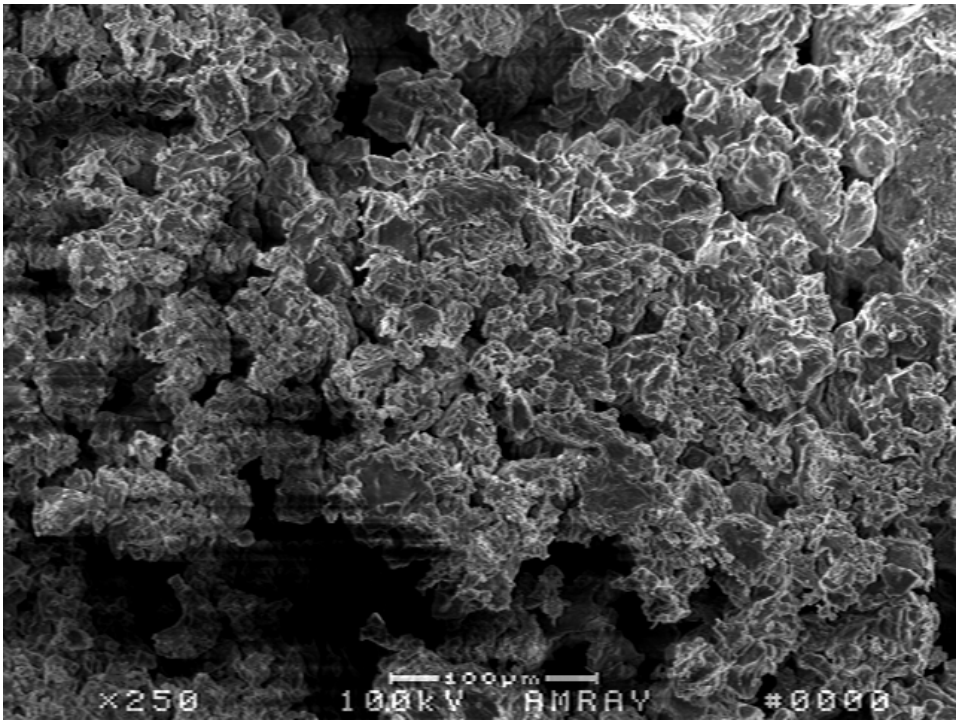

Figure 29: SEM image of 15m DM5 sample at 250x magnification (interior)

The microstructure of the dehydroxylated montmorillonite samples, presented in Figure 29, was the most disordered of the all 15m sample series. Pores are present, but are extremely irregular, varying in size from approximately 10-100 microns. This microstructure seems to

indicate these samples were only able to weakly react, forming only a sporadically linked polymer network. This conclusion is supported by the relatively low compressive strength and modulus observed during mechanical testing.

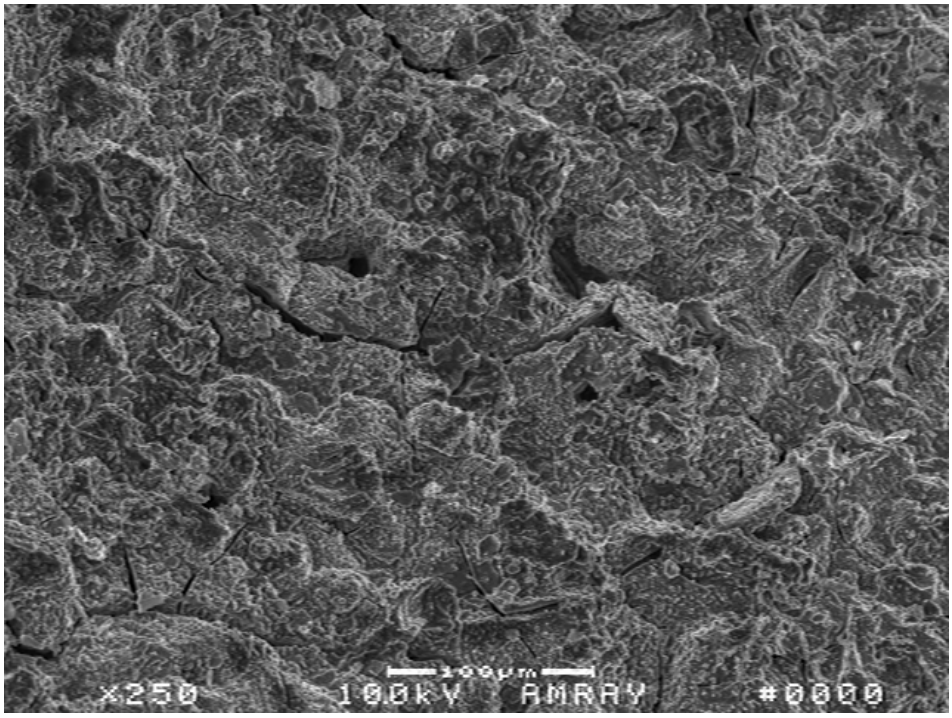

Figure 30: SEM image of 10m M5 sample at 250x magnification (interior)

Microanalysis of the 10m samples allowed observation of a very different microstructure than the samples made with 15m activating solution. As presented in Figure 30, these samples had very few pores present in the dried material. This indicates that the geopolymer gel either never fully formed due to the slow rate of reaction, or collapsed prior to the freeze drying process. This significant change in microstructure further explains the marked difference in mechanical properties observed between 10m and 15m samples.

Chapter 5:

Conclusions and Recommendations for Future Work

5.1 Conclusions

The goal of this work was to investigate a method to produce a low density alkali activated material which retains good compressive strength. A possible method for the production of an alkali activated aerogel material was presented. This method was investigated with several different sources of solid aluminosilicates and activating solutions. The materials produced by this method were evaluated based on their rheological development, FTIR spectra, compressive strength, elastic modulus, and microstructure.

This study shows that the production of an alkali activated aerogel is possible, with compressive strengths of up to 9.9 MPa, elastic moduli of up to 373 MPa, and densities as low as 0.8 $g \bullet cm^{-3}$. It is believed average density varied between compositions do to variations in size and amount of pores present in each composition. An increase in average density results in a reduction of air volume per bulk sample volume. Logically, this increase in solid polymer should improve the mechanical properties of the sample. This is confirmed by mechanical testing, where both compressive strength and elastic modulus were observed to vary inversely with average density.

Previous work suggests that a fully hardened alkali activated material could not be produced with low solid to activating solution ratios. Typical geopolymers have a solid to activator ratio between 1:1 and 2:1. Lower ratios were observed to separate into a biphasic mixture prior to the formation of a stable geopolymer precursor gel. In this work, a hardened alkali activated material is produced in samples with solid to activating solution ratios as low as 1:50. In these samples, gellation was induced through vigorous mechanical mixing. Mixing

increases the diffusion rate, causing an increase in the number of collisions between reactive monomers in the solution. This allows the solution to react more fully, producing a stable precursor gel in samples which would otherwise be too dilute to fully react.

The addition of sodium aluminate was observed to nearly double compressive strength in the S-type furnace slag samples. This addition of sodium aluminate to the activating solution causes an increase in the amount of aluminum ions available for incorporation into the geopolymer network, and therefore encourages the formation of more aluminosilicate bonds, improving the mechanical properties of the dried material.

The rheology data show that the time scale of the alkali activation and polymerization reactions are dependent on both the alkalinity of the activating solution used, and the choice of solid aluminosilicate. Activating solutions with increased alkalinity were found to decrease reaction times, both due to an increase in the rate of alkaline hydrolysis during the dissolution step and an increase in the proportion of low molecular weight silicates encouraged by the more alkaline environment. Of the solid aluminosilicates investigated, F-Type furnace slag was found to thicken fastest, with the dehydroxylated montmorillonite and metakaolin exhibiting significantly slower thickening.

Through FTIR analysis, it was shown that the slag and metakaolin both reacted to produce significant proportions of geopolymer bonds. This conclusion is drawn from the shift in the geopolymer main band to lower wave numbers, and the creation of a new absorbance peak from 630-760 cm^{-1},which is associated with the creation of geopolymer ring and cage structures. FTIR analysis of the alkaline activated dehydroxylated montmorillonite samples

showed relatively few changes from the spectra of the raw dehydroxylated montmorillonite in these bands. Therefore, it is believed that little geopolymerization occurs in the dehydroxylated montmorillonite samples under these conditions. This conclusion is supported by the generally poor mechanical properties observed in the dehydroxylated montmorillonite samples, and the disordered microstructure observed by SEM. However, an increase in the absorption band associated with Si-O-Si bonds can be observed in these samples. Therefore, the thickening and solidification of these samples is believed to be primarily a result of the formation of these silicone bonds.

5.2 Recommendations for Future Work

This study represents the preliminary steps in the formulation and evaluation of the novel use of freeze dry processing in the field of alkali activated materials. Due to time constraints, only one activating solution was investigated, at only two proportions of each solid aluminosilicate material. Some work in the field of geopolymers suggests the use of a potassium hydroxide and potassium silicate activator, rather than the sodium-based activator used herein, may produce faster reaction times and stronger materials. The use of greater amounts of solid aluminosilicate could also be investigated.

The silica to alumina ratio of alkali activated materials is known to be an important parameter relating to the mechanical properties of the cured material. In this study, reduction of the silica to alumina ratio through the addition of sodium aluminate was shown to greatly increase mechanical strength. Further investigation into the effects of the silica to alumina ratio through the addition of alumina, the reduction of silica in the activating solution, or the use of a different solid aluminosilicate would increase the understanding of the effects of this important parameter. Other solid aluminosilicates of interest include C-type fly ash, and various other mineral clays.

SEM observations indicate the presence of regular shaped, sharp deposits on the surface of the polymer network. It is believed these deposits are sodium and calcium formations left behind by the freeze drying process. However, further investigation is required to confirm this claim.

Another area of interest is the modification of the processing techniques used in this study to further reduce the bulk density of the final product. SEM observations confirm a closed microstructure on the surface of current samples. Performing maturation in a high-humidity environment to reduce evaporation and prevent gel collapse at the sample surface could result in faster and more complete drying of the material, resulting in a reduction in bulk density and processing time. Other process refinements, such as a longer freeze dry step or freeze drying at lower ultimate pressure, should also be investigated.

References

[1] Kistler, S. S. "Coherent Expanded Aerogels and Jellies" *Nature* Vol. 127 pp. 741, 1931 [8] Call, F. "Preparation of Dry Clay-Gels by Freeze Drying" *Nature* Vol. 172 pp.126, 1953

[2] Call, F. "Preparation of Dry Clay-Gels by Freeze Drying" *Nature* Vol. 172 pp.126, 1953

[3] Finlay, K. Gawryla, M.D. Schiraldi, D.A. "Biologically based fiber-reinforced/clay aerogel composites" *Ind. Eng. Chem. Res.* Vol. 47 pp. 615-619, 2008

[4] Davidovits, J. Geopolymer Chemistry and Applications 2nd Ed., Institut Geopolymere, St. Quentin France, 2008

[5] Bormans, P. "Ceramics are More than Clay Alone: Raw Materials, Products, Applications" Cambridge International Science Publishing, pp. 104-123, 2003

[6] van Olphen, H. An Introduction to Clay Colloid Chemistry 2nd Ed., Krieger Publishing Company, Malabar, FL, 1977

[7] Ishikawa, N. Fujii, K. Naoya, S. "The influence factor of structural change in kaolinite suspensions during a freeze-drying process" *Clay Science* Vol. 12 pp. 167-176, 2003

[8] Ishikawa, N. Fujii, K. Naoya, S. "The collapsing properties of kaolinite aerogels of dilute suspensions and analysis based on structure models" *Applied Clay Science* Vol. 38 pp. 146-152, 2007

[9] Somlai, L. S.; Bandi, S. A.; Schiraldi, D. A.; Mathias, L. J."Facile Processing of Clays into Organically-Modified Aerogels" *AIChE Journal* Vol. 52 No. 3 pp. 1162-1168, 2006

[10] Hofmann, U. *Nature* Vol. 171 pp. 682, 1953

[11] Arndt, E.M. Gawryla, M.D. and Schiraldi, D.A. "Elastic, low density epoxy/clay aerogel composites" *Journal of Materials Chemistry* Vol. 17 pp. 3525-2529, 2007

[12] Miller, S. Leventis, N. Johnston, C. J. Meador, M. "Clay Nanocomposite/Aerogel Sandwich Structures for Cryotanks" http://ntrs.nasa.gov/archive/nasa/casi.ntrs.nasa.gov/20060005182_2006005304.pdf

[13] Van Olphen, H. "Polyelectrolyte Reinforced Aerogels of Clays-Application as Chromatographic Adsorbents" *Clay Miner* Vol. 15 pp.423-435, 1967

[14] Duxsun, P.; Fernandez-Jimenez, A.; Provis, J.L.; Lukey, G.C.; Palomo, A.; van Deventer, J.S.J. "Geopolymer Technology: The current state of the art" *Journal of Material Science* Vol. 42, pp. 2917-2933, 2007

[15] Krivenko, P. V.; Shi, C.; Roy, D.; Alkali-Activated Cements and Concretes 1st Ed. Taylor & Francis, New York, NY, 2006

[16] MacKenzie, K.J.D.; Komphanchai, S.; Vagana, R.; "Formation of inorganic polymers (geopolymers) from 2:1 layer lattice aluminosilicates" *Journal of the European Ceramic Society* Vol 28 pp.177-181, 2008

[17] Provis, J. L., van Deventer, J. S. J. "Geopolymerisation kinetics. 1. In situ energy-dispersive X-ray diffractometry" *Chemical Engineering Science* Vol. 62, pp.2309-2317, 2007

[18] Provis, J. L., van Deventer, J. S. J. "Geopolymerisation kinetics. 2. Reaction kinetic modeling" *Chemical Engineering Science* Vol. 62, pp.2318-2329, 2007

[19] Rees, C. A., Provis, J. L., Lukey, G. C., van Deventer, J. S. J."The mechanism of geopolymer gel formation investigated through seeded nucleation" *Colloids and Surfaces* Vol. 318 pp. 97-105, 2008

[20] MatWeb Material Property Data, "Portland Cement" <http://www.matweb.com/search/DataSheet.aspx?MatGUID=bef6d86a5fe94c91b2300ed172e2a1f4&ckck=1>, 17 July 2008

[21] Liefke, E.; "Industrial Applications of Foamed Inorganic Polymers" Geopolymer '99 Proceedings, pp 189-199, 1999

[22] Bell, J. L.; Kriven, W.M.; "Preparation of Ceramic Foams From Metakaolin-Based Geopolymer Gels" In Developments in Strategic Materials. Edited by Hua-Tay Lin, Kunihito Koumoto, Cer. Eng. Sci Proc. Vol 29 [10] pp. 97-112, 2008

[23] Lee, W. K. W.; van Deventer, J. S. J.; "Use of Infrared Spectroscopy to Study Geopolymerization of Heterogeneous Amorphous Aluminosilicates" *Langmuir* Vol 19 pp. 8726-8734, 2003

[24] Rees, C. A.; Provis, J.L.; Lukey, G.C.; van Deventer, J.S.J.; "Attenuated Total Reflectance Fourier Transform Infrared Analysis of Fly Ash Geopolymer Gel Ageing" *Langmuir* Vol 23 pp. 8170-8179, 2007

[25] Rees, C. A.; Provis, J.L.; Lukey, G.C.; van Deventer, J.S.J.; “In Situ ATR_FTIR Study of the Early Stages of Fly Ash Geopolymer Gel Formation” *Langmuir* Vol 23 pp. 9076-9082, 2007

[26] Heller-Kallai, L.; Lapides, I.; "Reactions of Kaolinites and Metakaolinites with NaOH—comparison of different samples (Part 1) " Applied Clay ScienceVol. 35 pp. 99-107, 2007